catalysts

MDPI

Review

A Review on Production and Surface Modifications of Biochar Materials via Biomass Pyrolysis Process for Supercapacitor Applications

Rifat Mehdi [1], Asif Hussain Khoja [2,*], Salman Raza Naqvi [1,*], Ningbo Gao [3] and Nor Aishah Saidina Amin [4]

[1] School of Chemical & Materials Engineering (SCME), National University of Sciences and Technology (NUST), Sector H-12, Islamabad 44000, Pakistan; rmehdi.phdscme@student.nust.edu.pk
[2] Fossil Fuels Laboratory, Department of Thermal Energy Engineering, U.S.-Pakistan Centre for Advanced Studies for Energy (USPCAS-E), NUST, Sector H-12, Islamabad 44000, Pakistan
[3] School of Energy and Power Engineering, Xi'an Jiaotong University, Xi'an 710049, China; nbogao@xjtu.edu.cn
[4] Chemical Reaction Engineering Group (CREG), School of Chemical & Energy Engineering, Faculty of Engineering, Universiti Teknologi Malaysia (UTM), Johor Bahru 81310, Malaysia; noraishah@cheme.utm.my
* Correspondence: asif@uspcase.nust.edu.pk (A.H.K.); salman.raza@scme.nust.edu.pk (S.R.N.)

Abstract: Biochar (BC) based materials are solid carbon enriched materials produced via different thermochemical techniques such as pyrolysis. However, the non-modified/non-activated BC-based materials obtained from the low-temperature pyrolysis of biomass cannot perform well in energy storage applications due to the mismatched physicochemical and electrical properties such as low surface area, poor pore features, and low density and conductivity. Therefore, to improve the surface features and structure of the BC and surface functionalities, surface modifications and activations are introduced to improve its properties to achieve enhanced electrochemical performance. The surface modifications use various activation methods to modify the surface properties of BC to achieve enhanced performance for supercapacitors in energy storage applications. This article provides a detailed review of surface modification methods and the application of modified BC to be used for the synthesis of electrodes for supercapacitors. The effect of those activation methods on physicochemical and electrical properties is critically presented. Finally, the research gap and future prospects are also elucidated.

Keywords: biomass; pyrolysis; biochar production; surface modification; supercapacitor

check for updates

Citation: Mehdi, R.; Khoja, A.H.; Naqvi, S.R.; Gao, N.; Amin, N.A.S. A Review on Production and Surface Modifications of Biochar Materials via Biomass Pyrolysis Process for Supercapacitor Applications. *Catalysts* **2022**, *12*, 798. https://doi.org/10.3390/catal12070798

Academic Editor: Tomás García

Received: 28 May 2022
Accepted: 12 July 2022
Published: 20 July 2022

Publisher's Note: MDPI stays neutral with regard to jurisdictional claims in published maps and institutional affiliations.

Copyright: © 2022 by the authors. Licensee MDPI, Basel, Switzerland. This article is an open access article distributed under the terms and conditions of the Creative Commons Attribution (CC BY) license (https://creativecommons.org/licenses/by/4.0/).

1. Introduction

Increasing population, energy demands, and depletion of natural non-renewable energy resources like coal, gas, and petroleum threaten the energy security of the planet [1]. It is very important to develop cheap and good environmental solutions to address these energy-related problems. In this regard, energy storage and conversion from renewables like biomass can be the right alternate to solve energy requirements [2,3]. For energy storage, there is the development of low cost material to be synthesized from the abundantly available renewables and natural resources like lignocellulosic biomasses [4].

Sustainable energy generation requires efficient energy storage equipment to harvest energy [5]. Among those storage equipment, lithium-ion batteries attracted much attention due to their high energy density. Short life, low power density, and high cost are the issues associated with lithium-ion batteries [6]. Therefore, it is required to develop a device with better energy storage performance. Supercapacitors gained interest for being a promising energy storage device for the future due to their fast charge/discharge rate, high power density, and good cycle stability [7]. However, due to their lower energy density, they are not widely used in the energy storage market. Researchers are working to develop such energy storage materials to achieve promising performance in energy applications [8]. In

order to evaluate the performance of the supercapacitor, the basic elements related to the electrodes and electrolyte are considered [9]. The capacitive performance of electrodes are highly desirable and can be increased with the help of stable, long lasting, and electrically conductive electrode material. These properties along with surface wettability are of prime importance while fabricating the electrode materials [10]. Carbon materials obtained from biomass have been considered as suitable materials for supercapacitors because of their physicochemical properties like high surface area, high porosity, electrical conductivity, functional groups, availability of metal ions and minerals, stable structure against electrochemical activity, and their morphology for ions mobility [11,12].

Lignocellulosic biomass provide the chemically stable, tunable pore structure, and high surface area carbonaceous material. Due to these properties, the lignocellulosic biomass is advantageous over the other material for the application of high electrical conductance [13]. The carbon materials produced from biomass have attracted much attention due to their environmental friendly nature, natural abundance, and special porous features in energy storage and conversion applications [14]. Biochar (BC)-based materials played a vital role in energy storage and conversion, including making electrodes for supercapacitors [15], electro-catalysts [16], and lithium-ion batteries. Conventional carbon materials mainly obtained from the non-renewable sources require severe production conditions and synthesis method [17]. Hence, in order to adopt environment friendly methods of producing carbon-based material, a sustainable source of raw material needs to be adopted for positive prospects. In order to produce BC-based material, the promising raw material can be the biomass that has an inherent potential content of 45 to 50 wt% carbon [18]. Lignocellulosic biomass is composed of cellulose (40–50 wt%), hemicelluloses (15–30 wt%), and lignin (15–30 wt%) [19]. The composition of biomass indicates the decomposition of contents at temperatures that are lower than 500 °C. This feature exists due to the presence of lignin, cellulose, and the hemicellulose in biomass. This biomass can easily be decomposed to produce BC, bio-oil, and incondensable gases, which are a direct result of pyrolysis at low temperature. However, BC materials show poor capacity retention and lower specific capacitance due to poor pore features and lower surface area. The BC materials with pre- or post-treatment show promising results of electrochemical applications. A higher pyrolysis temperature and treated BC can present the correct pore properties and electrochemical applications [20]. Inadequate pore structure and poor size distribution in BC-based materials greatly affect the performance of supercapacitors. These green pyrolyzed biomass materials exhibit an amorphous structure, which lowers their electrical conductivity and also affects the performance of supercapacitors. Due to the carbonization temperature, aromatic carbon contents increase with the significant loss of surface functionalities like carboxyl, carbonyl, and hydroxyl [21]. BC, having physicochemical properties like high porosity, functional groups, superior stability, a large surface area, availability of metal cation and minerals, and high cation exchange capacity can be a promising candidate for energy and environmental applications [12]. These physicochemical properties can be modified according to the required electrochemical applications. Therefore, to tailor the structure of the BC, surface functionalities and activation should be introduced by different surface modification methods to obtain an excellent energy storage material for supercapacitors.

Previously different modifications were reviewed separately. Babasaheb M. Mastagar et al. [22] reviewed the biomass-derived nitrogen-doped porous carbon and its various applications like catalysis and electrochemical energy storage. Baharak Sajjadi et al. [23,24] presented a review article studying the physical action and chemical activation of BC for environment and energy sectors. Wei-Hao Huang et al. [25] updated the research efforts for BC modifications, particularly to the end applications based of physical and chemical activation. Feng Shen et al. [26] updated mechanisms that are employed in order to value add the carbon materials in the context of mechano-chemical conversion. Emanuela Calcio Gaudino et al. [27] studied the sono-chemical and mechano-chemical surface modification techniques to valorize the biomass. However, there is no review that discusses the surface

modification techniques to produce surface modified BC-based material with desired surface features to achieve the excellent performance in supercapacitors application. Therefore, the objective of this work is to provide a state of the art review on BC production via pyrolysis, surface modification, and application for supercapacitors to store energy.

In this review, the BC production via the pyrolysis of biomass and its surface modification is exclusively discussed. The surface modification techniques for activating the BC (physical activation, chemical activation, and physicochemical activation), metal loading on the BC's surface, heteroatoms doping on the surface of BC, sono-chemical and mechanochemical modifications are critically discussed. The application of modified BC-based materials in supercapacitor applications is briefly presented. Moreover, the research gap for future directions and recommendations were also presented.

2. Overview of Biomass Pyrolysis for BC Production

Pyrolysis is one of the thermo-chemical conversion methods used to decompose biomass into useful products in a limited supply of oxygen or in an inert environment that does not allow gasification to some extent. Pyrolysis is carried out at temperature ranging from 300–650 °C for a specific time interval to produce non-condensable gases, solid char, and liquid products [28]. BC is a solid carbonaceous material produced via different thermal techniques along with liquid and gas as valuable products from widely available biomass feedstocks. During BC production via pyrolysis, biomass undergoes a set of complex reactions. To restructure the morphology, porosity, and functionality of the biomass-derived BC, it is very important to understand these reactions [29]. In pyrolysis the degrees of polymerization is an important factor in the reaction mechanism of pyrolysis [30]. These reactions are affected by key constituents of the employed biomass, which include lignin, cellulose, and hemicellulose. During pyrolysis, these components decompose at different temperature zones for disintegration to produce the porous carbonaceous material. The pyrolysis process has successive stages for the conversion and disintegration of biomass. The initial process is the removal of the absorbed moisture, which takes place at a temperature of about 100–150 °C, and the degradation of hemicellulose that occurs from 150–260 °C. Afterwards, the cellulosic decomposition range is from 240–350 °C, and finally, in the case of lignin, the decomposition takes place at about 280–500 °C [28]. Thus, during pyrolysis process de-volatilization of volatiles–which constitutes of carbon monoxide, carbon dioxide, and methane–takes place to produce BC and black solid, which is majorly solid carbon. As biomass has complex physical and chemical properties and structure, the produced carbonaceous material possesses poor surface structure. However, these carbon materials can be employed for different applications like batteries, capacitors, and soil and environmental remediation. Consequently, these resultant BC-based materials require surface modification for activation, which need to bear the controlled attributes of surface chemistry, porosity, surface area, and stability. Primarily, the biomass has cellulose, hemicellulose, and lignin as constituents. These components of biomass provide a strong rigid structure to plants due to chemical bonds [31]. Pyrolysis of biomass is performed under an inert atmosphere in the temperature range of 350–700 °C [32]. The operating conditions such as heating rate, temperature, and residence time greatly influence the distribution of the products. A lower heating rate, long residence time, and lower pyrolysis temperature (slow pyrolysis) favors the production of char, while a relatively higher temperature, short residence time, and higher heating rate (fast pyrolysis) promotes the oil yield [33]. However, the increased temperature could lead to cracking of the volatile, thereby enhancing the yield of on-condensable gases. The operating conditions in pyrolysis experiments can be optimized depending on the desired products.

Effective energy storage applications can be manifested by producing BC from biomass, employing the pyrolysis process and modifying the surface via activation. This modification is an efficient approach to store energy. BC-based materials have well developed pore structure and functional groups, hence the selection of correct material is important in order to employ the precursor to obtain the desired attributes for enhanced applicability.

Biomass precursors for BC production should be cheap, abundant, renewable, diverse, and environment friendly. To obtain the desired surface and textural properties, higher fixed carbon is imperative in the biomass along with the lowest possible ash contents [34]. A vast variety of biomass is available, such as woody and non-woody biomass, industrial waste biomass, and agricultural biomass wastes to be considered for the selection of the precursor with which to produce BC-based materials. The physicochemical properties of biomass for BC-based material production are based on elemental composition, proximate analysis, particle size, grindability, and density of the biomass. Lignocellulosic biomass contains mainly carbon, hydrogen, oxygen, nitrogen, calcium, potassium, and minor concentration of Si, P, Al, Mg, and Fe, etc. Due to some of the constraints like high moisture content, low bulk density, diverse physicochemical properties, and seasonal variation, lignocellulosic biomasses are not used as a direct energy conversion source [35]. For thermochemical conversion to make biochar, it is necessary to understand the chemical composition of biomass. The components in lignocellulosic biomass such as hemicellulose, cellulose, and lignin have certain decomposition temperature and degradation rates. Hemicellulose decomposition starts earlier than for cellulose and lignin. Generally, hemicellulose produces lower char, tar, and gas [36,37], while lignin produces higher char and less gases compared to cellulose. Cellulose has been reported to produce higher oil yield and lower gases and char yield [36,37]. Cotton stalk has lower hemicellulose (27.98%) and lignin (20.51%) contents, which promotes less char yield, while the cellulose content of 40.17% promotes a higher production of oil [38]. The hemicellulose and lignin content of biomass are critical compositional parameters for char production. The feedstocks with higher lignin content have been reported to produce higher char yield compared to those with higher hemicellulose content. Khan et al. [39] investigated the pyrolysis of rice straw and waste tire at 550 °C in a fixed bed reactor. The char yield from the pyrolysis of rice straw alone was slightly lower than the oil yield, which corresponds to the lower lignin content. Moreover, Ma et al. [40] reported that the char obtained from lignin is superior to char derived from hemicellulose in the terms of mass and energy yield. However, the surface structure and porosity of the char derived from cellulose is superior compared to that of lignin. Lignin, due to its complex structure, degrades at a wide range of temperature ranging from 150–900 °C, and has a complex degradation mechanism that causes a lower surface area and total pore volume [41]. It was also found that the higher the lignin content, the higher the surface area and porosity, which is due to the stable structure of lignin and preserved pore structure [42,43]. Similarly, the feedstocks with higher fixed carbon content will produce a higher char yield compared to those with higher volatile contents. The ash content is another compositional parameter of feedstock that significantly impacts the quality of char. Char with a lower ash content renders higher porosity, and a higher ash content causes a lower surface area as ash blocks the pores of biochar, which restricts its performance in supercapacitor applications [44].

Figure 1 shows factors affecting the pyrolysis process, subsequently on the physicochemical and electrical properties of BC. For instance, various factors have been studies and found a great impact on the properties and production of BC, which include the reaction temperature, heating rate, and nature of the feedstock as major influencers [45]. The composition of biomass has a promising impact on the yield of the pyrolysis process, especially its hydrogen-to-carbon (H/C) and oxygen-to-carbon (O/C) ratio. With components of lignocellulosic biomass, each one has its own decomposition temperature range like hemicellulose (150–350 °C), cellulose (275–350 °C), and lignin (250–500 °C) [46]. The particle size of the biomass feedstock has an effect on the products of the pyrolysis process. The smaller the particle size, the higher the liquid yield, as it offers less resistance to the release of condensable gases. On the other hand, a bigger particle size resists the primary product of pyrolysis, which favours secondary cracking to yield solid product. The pyrolysis reaction temperature is the parameter that can affect yield, as well as physical and chemical properties of the BC. Previously, achnatherum was pyrolyzed at 300 °C, 500 °C, and 700 °C, which enunciated a decrease in BC yield from 48% to 24% with an increasing

reaction temperature, which further resulted in the gradual disappearance of the functional groups on the BC [47]. Pyrolysis temperature has a prominent impact of the surface area and total pore volume. At lower temperatures of less than 400 °C, only a slight change occurs as it does not provide appropriate conditions for complete devolatilization, which restricts the formation of new pores [48]. As the temperature rises, the amorphous carbon changes to crystalline and higher temperature also provides activation energy, which leads to micropore formation [49].

The heating rate has a remarkable effect on the surface features and yield of the BC. BC yield is increased at low heating rates because the decomposition of the biomass is lowered during the secondary cracking process. The formation of aromatic structures in BC occurs at lower heating rates rather than at a fast heating rate [50]. The heating rate has a very close relation to BC-specific surface area and porosity. For instance, when the heating rate was increased from 1 °C/min to 20 °C/min, the surface area of rapeseed stem-derived BC was increased from 295.9 m^2/g to 384.1 m^2/g, while the pore volume was increased from 0.1659 cm^3/g to 0.2192 cm^3/g [51]. In another study, it was found that when the heating rate was increased from 10 °C/min to 30 °C/min, the surface area was found to be increased from 210.4 m^2/g to 411.06 m^2/g, but it was decreased to 385.38 m^2/g when the heating rate was further increased to 50 °C/min [52]. From the previous studies, a conclusion can be drawn that a suitable and preferable surface area and porosity of biochar can be achieved at heating rate from 5 °C/min to 30 °C/min. Residence time also has a great influence on the surface area and porosity of the BC. In addition, it was also studied that surface area of rapeseed stem-derived BC increased from 46.7 to 98.4 m^2/g against the residence time increasing from 10 min to 60 min, but the surface area decreased to 91.4 m^2/g when the residence went to 100 min. Prolonged residence time and exposure to high temperature leads to the destruction of pores, therefore, a residence time in the range of 30–120 min is generally considered appropriate [51]. During pyrolysis, nitrogen gas is generally used, which has an important impact on the surface properties of BC. The surface area and pore volume increase with the increase in the flow rate of N_2 gas during pyrolysis. Previous study shows that the surface area of BC increased from 36 m^2/g to 352 m^2/g against the respective gas flow rates of 50 to 150 mL/min [53]. Devolatilization increases with the increased flow of gas, which causes pore formation to increase the surface area [54]; however, a flow rate that is too high leads to less release of volatile matter, which indicates a lower surface area and pore volume [53].

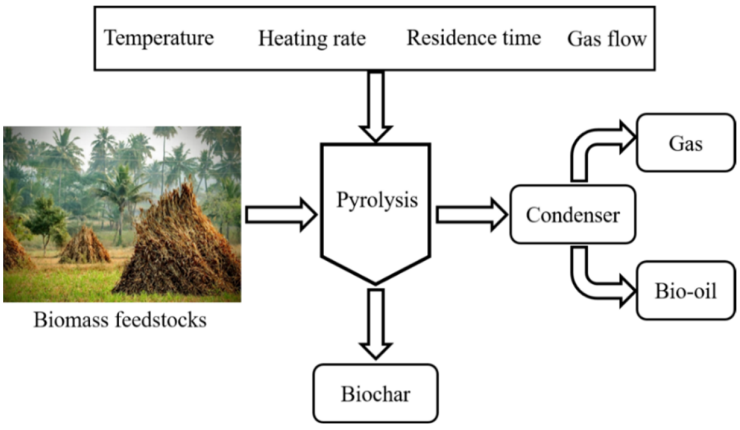

Figure 1. Factors affecting the pyrolysis process of biomass. Recreated with permission from Ref. [55]. Copyright © 2022 Springer Nature.

Based on heating rates, residence time, and heating methods, pyrolysis can be broadly categorized into slow pyrolysis, fast pyrolysis, flash pyrolysis, and microwave-assisted pyrolysis. The product of the pyrolysis process mainly depends on the reactor design, characteristics of the biomass–either physical or chemical, and operating parameters.

A long residence time (hours to days), low heating rate, and pyrolysis reaction temperature range for slow pyrolysis is 400 °C to 600 °C, and it was concluded that 600 °C was the most effective temperature to obtain a high surface area (261.78 m^2/g and 307.10 m^2/g), total pore volume (0.16 cm^3/g and 0.18 cm^3/g), high mass fraction (84.87 and 88.43 wt%), and carbon and fixed carbon (84.07 and 85.16 wt%) for the biomass materials pigeon pea stalk and bamboo, respectively [56]. Slow pyrolysis yields higher BC with less carbon contents, while fast pyrolysis favors a higher heating value, specific surface area, and carbon contents with a smaller yield of BC [57]. Some of the factors affecting the physiochemical properties of BC produced via pyrolysis are previously reported in [49,58].

Briefly, pyrolysis biomass is heated so swiftly that it reaches pyrolytic temperature before it decomposes. A very high heating rate 10–200 °C/s, pyrolysis temperature in the range of 425–600 °C with a short residence time 0.5–10 s, and maximum liquid yield up to 50–75% are the important features of fast pyrolysis [59], while flash pyrolysis is characterized by a higher heating rate that may reach 2500 °C/s and a short residence time of <0.5 s with a bio-oil yield of up to 75–80%. In microwave pyrolysis, microwaves are used to generate heat inside the feedstock samples without any contact between the sample and heating source as in conventional pyrolysis [60,61]. Microwave pyrolysis, due to uniform heating, is more efficient than conventional pyrolysis. In conventional pyrolysis, uneven heating leads to a degraded quantity and quality of the bio-oil, while uniform heating in microwave pyrolysis yields a superior bio-oil with better chemical composition [60]. Figure 2 shows the heating patterns of microwave-assisted pyrolysis and conventional pyrolysis [62]. In conventional pyrolysis, the sample is heated by convective heat transfer from the surface to the core, while the microwave sample is heated from the core to the surface.

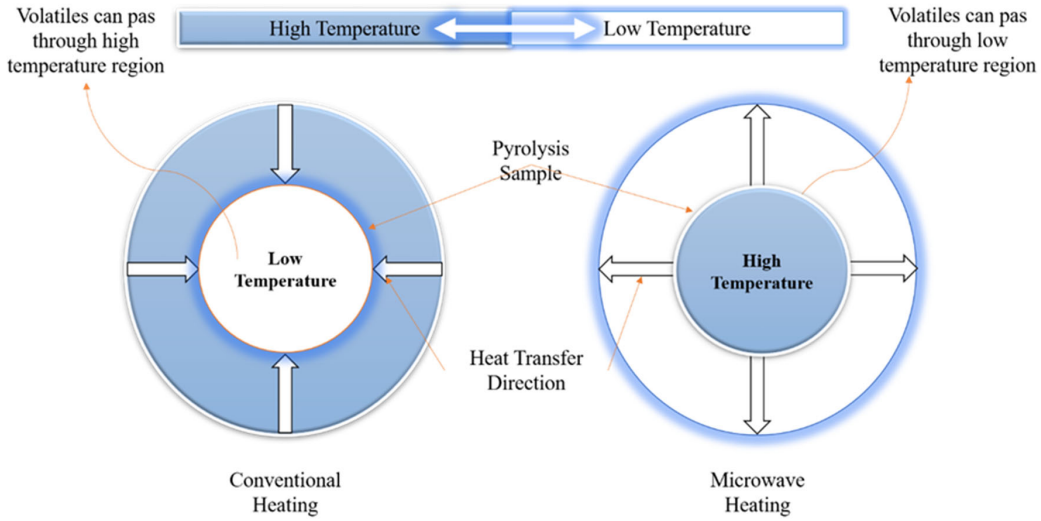

Figure 2. Comparison of microwave pyrolysis with the conventional pyrolysis of biomass. Recreated with permission from Ref. [62]. Copyright © 2003 Elsevier B.V.

BC-based materials obtained from different biomass feedstocks like wood, plant waste, agro-residues, and industrial biomass waste have been used to develop electrodes for supercapacitors applications. BC-based materials are attractive for supercapacitors applications due to their physicochemical properties such as low cost, abundant availability, high thermal stability, compatibility to be transformed to composite and hybrid materials, good corrosion resistance, and easy processability [63]. However, issues associated with these materials are obtaining a suitable surface area with a desired pore structure, high electrical conductivity, and good compatibility with electrolyte solution [64]. As reported above, BC-based materials obtained from lignocellulosic biomass feedstocks have abundant oxygenated functional groups compared to conventional carbon materials. These oxygen contents can be tuned by different pyrolysis conditions like the heating rate, residence time,

and pyrolysis temperature. Some BC-based materials have a very small surface area and limited developed porosity that can be evaded by producing stable, highly porous BCs, which are a result of the various activation methods [65]. To address these issues, different surface modification techniques are being used to elevate the values of specific capacitance and porosity. This can further improve the surface features of produced BC-based materials for high-performance supercapacitors [64].

3. Surface Modification of BC for Supercapacitor Applications

Carbon-based electrodes bearing functional groups on the surface, in addition to the pore network, distribution, specific surface area, metal oxides and the hetero-atom, are the key attributes that regard the elevated performance of the electrochemical devices [66,67]. Elevating these properties would mean enhancing the electrochemical ability of the produced anode material. Various methods are applicable in order to modify the pore structure, surface chemistry, and specific surface area of these produced carbonaceous materials. These methods can be either physical or chemical and are being widely used [68]; corn husk-derived BC was produced by chemical modification using KOH as an activating agent with an enhanced surface area of 928 m^2/g and specific capacitance of 356 F/g. BC surface features can be modified to enhance its performance in several applications by different methods. Figure 3 displays that modification can be either made with pre-treatment, post treatment, or self-activation mods [25]. In route 1, Q Sun et al. [69] pretreated cotton biomass with magnesium nitrate, followed by carbonization and activation using $ZnCl_2$ as an activating agent at 800 °C for 2 h in a tube furnace under N_2 gas flow to produce surface-modified BC for a supercapacitor. Results showed a high surface area of 1990 m^2/g and capacitance of 240 F/g with 89% cycle stability. In route 2, L Qin et al. [70] reported the post treatment of pine nut shell to make surface-modified activated carbon for application in supercapacitors, adopting the steam activation method. In route 3, Z Zhang et al. [71] reported the self-activation of biomass (Glebionis coronaria) to produce surface-modified carbon electrodes that have nitrogen doped on their surface for possible application in supercapacitors [71]. In addition, Glebionis coronaria-derived BC achieved a specific capacitance of 205 F/g with a capacitance retention up to 95% after 5000 cycles and an enhanced surface of 1007 m^2/g.

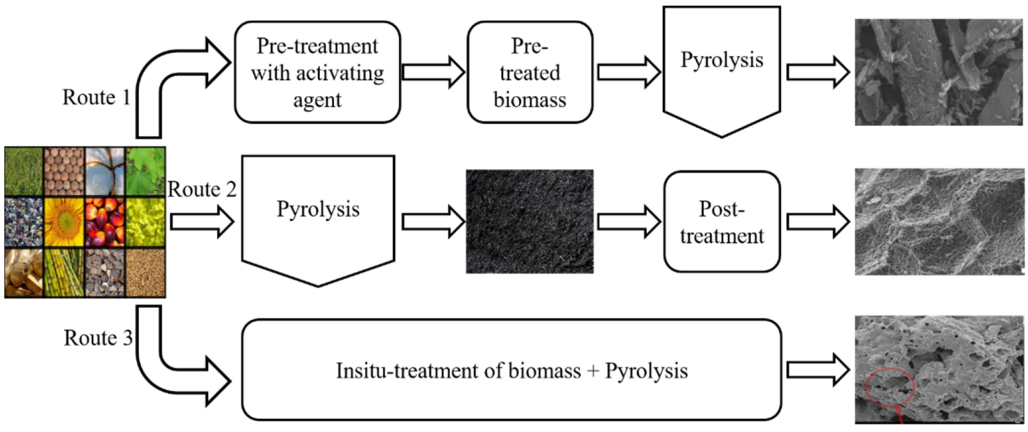

Figure 3. BC surface modification by different routes. Route 1: pretreatment method [69], Route 2: post treatment method [70], Route 3: self-activation [71]. Recreated with permission from Ref. [25]. Copyright © 2020 Elsevier B.V.

On a broader spectrum, five main techniques are used to modify the structure and surface functionalities of BC. These can be either applied pre or post pyrolysis. These include the activation of BC, doping of heteroatoms on BC, loading of metal oxides on BC, and mechanochemical and sono-chemical surface modification of BC.

3.1. BC Activation Methods for Supercapacitor Applications

BC-based materials directly obtained from pyrolysis generally present poor surface attributes and lower SA; these properties like improved energy density, rapid charge discharge are critical to the electro-chemical applications, while activation enhances the surface features of activated carbon [72]. The activation of BC involves two steps: one is pyrolysis of the biomass selected, and the second is the surface modification carried out with the help of activation. Pyrolysis produces a BC with a pore structure that is not fully developed and a stable structure that can be restructured by chemical or physical activation methods. Physically activated carbon from oil palm fruit demonstrated a larger porosity and higher surface area compared to raw BC [73]. Physicochemical activation is another plausible solution to modify the surface of the BC in order to enhance the properties of the activated carbon [74,75]. The method via which the physicochemical properties of BC are altered is crucial. Ranging from physical and chemical, this method can also be the physical–chemical treatment. Figure 4A–C shows the AC with diverse morphologies produced via these techniques. Katarzyna Januszewicz et al. [76] employed physical and chemical methods and prepared activated carbon from chestnut shells. E. Taer et al. [74] synthesized AC and employed it for supercapacitor applications; sugarcane bagasse was the biomass that was treated, using a combination of physical and chemical activation processes for effective surface results as can be seen in Figure 4C. The cyclic voltammetry showed that both cells showed the same rectangular shapes in the potential range. An increase in current values was evident in the combination of physically and chemically activated BC.

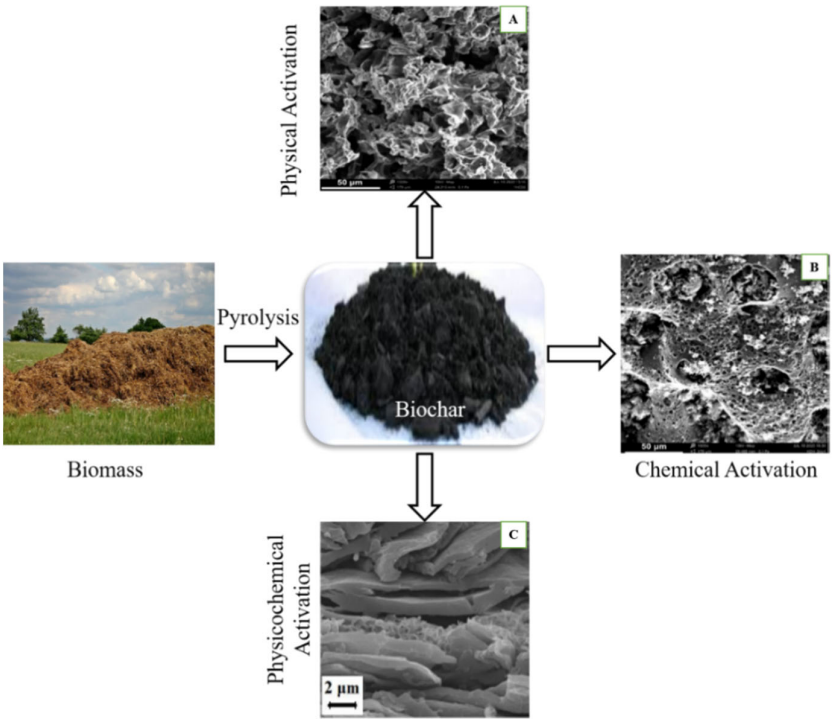

Figure 4. SEM images of activated carbon production via physical, chemical, and a combination of both physical and chemical activation. (**A**) Physical activation; (**B**) chemical activation, adopted with the permission from Ref. [76]. Copyright © 1996-2020 MDPI (**C**) physicochemical activation. Reproduced with the permission from Ref. [74]. Copyright © 2014 Trans Tech Publications.

Table 1 summarizes the three activation methods, which include physical, chemical, and physicochemical activation methods [77]. Many lignocellulosic biomass feedstocks that include husks, roots, shoots, shells, etc., are listed. Different types of activation agents including acids, alkali, and salts can be used for chemical activation. For physical activation, air, steam, and CO_2 are the main agents used for activation.

Table 1. Activation methods, chemical activation, physical activation, and physicochemical activation to produce activated carbon from different biomass feedstocks using different activation agents. Adapted with permission from Ref. [77].

Method of Activation	Lignocellulosic Biomass	Activation Agent	Ref.
Physical activation	Coffee endocarp, rice husk fly ash, sawdust fly ash, corncob, macadamia nut shell, bagasse bottom ash, date stones	CO_2 and steam	[78–80]
	Bean pods, coconut shell, olive stones, apple pulp, coffee endocarp	Steam/CO_2	[81–84]
	Vine shoots, sugarcane bagasse	CO_2 and air	[48,85]
	Pine nut shell	Steam	[70]
Chemical activation	Fish skin, onion, palm kernel shell, bamboo species, argan (Argania spinosa) seed shells, potato starch, goat hair, coconut shell, soybean oil cake, distillers dried grains, elm samara, cornstalk	KOH	[86–101]
	Silkworm excretment, of squid gladius chitin, wax ground, cuttle bones, wheat straw, rice straw, cotton stalk, soybean stalk, peanut shell, banana peel, polysaccharides	NaOH, and NaOH/KOH	[102–107]
	palm kernel shell, cashmere, cocoa pod husk	KOH/K_2CO_3	[89,108,109]
	Shrimp shell, waste particleboard, wood waste sticks	H_3PO_4/KOH	[82,84,110]
	teakwood sawdust, potato waste, S. bengalense, residue, Persian ironwood	$ZnCl_2$	[111–113]
	Raw cotton, bean curd	$Zn(NO)_3$ and CH_3COOK	[114,115]
Physicochemical activation	Peanut shell	KOH and air	[116]
	Needle coke	Steam	[117]
	Cassava peel waste	KOH and CO_2	[118]

3.1.1. Physical Activation for BC Modification

Physical activation of BC is a process involving two steps. Firstly, the carbonization of biomass feedstock takes place at higher temperatures of <800 °C. In the second step, this produced carbon is activated by using suitable activating agents. These agents can be air, CO_2, and steam at higher temperatures [119]. Among these activating agents, CO_2 is superior to others due to its lower reactivity at high temperatures and controllability of pore structure [120,121]. Hybrid willow, a lignocellulosic biomass was converted to AC via physical activation using CO_2 as an activating agent. Maximum specific capacitance was achieved up to 92.7 F/g at a current density of 100 mA/g. A temperature of 800 °C and 60 min residence time was the optimum activation condition to achieve the maximum surface area of 738.74 m^2/g. [122]. It is usually carried out at lower temperatures in the air, while at a temperature range from 700 °C to 1100 °C in steam and CO_2 [62]. However, a temperature of 1200 °C and above leads to a lower carbon yield, ash formation, and collapse of the pore structure [123]. On the other side, the devolatilizion process happens to increase pore making in order to enhance the capacity of the BC [124]. This activation method is highly adoptable and environmentally friendly, but the correct proportions of speed, time, and temperature are crucial. In order to establish the required surface properties and creation of functional group activation, the temperature and duration must be appropriate as BC obtained by this method of activation is mainly affected by time and

temperature [125]. BC and H_2O or CO_2 react during physical activation, causing carbon atoms to be removed with the formation of pore structures, represented by Equations (1)–(3) [126,127].

$$C + CO_2 \rightarrow 2CO \quad (1)$$

$$CO + H_2O \leftrightarrow CO_2 + H_2 \quad (2)$$

$$C + H_2O \rightarrow H_2 + CO \quad (3)$$

Syzygium cumini fruit shells (SCFS) along with another biomass–Chrysopogon zizanioides roots (CZR)–are biomass precursors used to make activated carbon denoted by (SCFS-AC) and (CZR-AC), respectively, which are employed for supercapacitors. The BC for these materials was produced by the method of physical activation. SCFS-AC and CZR-AC symmetric supercapacitors exhibited the extraordinary values of the capacitance of 253 F/g and 294 F/g at 0.5 A/g, respectively. However, SCFS-AC delivers a specific capacitance of 120 F/g at a high current density of 10 A/g due to its high surface area and good distribution of microspores and the thick pore walls of its surface, indicating good stability, while CZR-AC showed a specific capacitance 50 F/g at 5 A/g current density with a mesoporous distribution and thin walls, indicating less stability than SCFS-AC [128]. Activated porous carbon (PAC) electrode material from pine nut shell was produced via steam activation. Effects of factors affecting the properties were analyzed. These are the activation time, temperature, and steam flow rates. The optimal conditions were a temperature of 850 °C, time of 60 min, and 18 mL/h of steam flow indicated by PAC850-60-18. Figure 5a represents the crystallinity and functional groups of BC produced from pine nut shell denoted PNSB and activated carbon at optimized conditions that were analyzed by XRD [70]. The pattern showed that both have diffraction peaks at 43° and 23°, respectively, which are amorphous structures. The peak intensity of activated carbon is slightly higher, which indicates that activation can enhance the degree of graphitization. Figure 5b,c depicts the obtained AC showed a specific capacitance of 128 F/g at a current density of 0.5 A/g and specific surface area of 956 m^2/g. Figure 5d shows the SEM micrograph of the activated carbon produced at optimum conditions at a higher magnification. It shows the uniformity and developed pore structure with micropores, mesopores, and macropores [70]. Chestnut seed-derived activated carbon was obtained via physical method of activation by CO_2 and chemical activation by KOH as an electrode material to achieve the specific surface area of 1221.2 m^2/g in the case of chemical activation, while 105 m^2/g and the capacitance of 173 F/g at 0.1 A/g with physical activation. The power density of 2030 W/kg with the energy density of 3.12 Wh/kg clearly indicates that the obtained activated carbon is a promising material for use in applications of supercapacitors [76]. The physical activation technique is much more advantageous compared to other techniques due to its commercial scale application and adaptability. The resulting BCs also show promising properties of enhanced porosity and physical strength [96,129], but a low BC yield, longer time of activation, higher activation temperature, and high energy consumption to carry out the activation process are the major concerns associated with physical activation.

Hemp fiber biomass precursor was used to synthesize hemp fiber porous carbon (HFPC) by physical activation using CO_2 as an activating agent. Duration activation was studied for 10 h, 20 h, and 30 h, representing the samples as HFPC-10, HFPC-20, and HFPC-30, respectively. Figure 6a–c shows the images of the field emission scanning electron microscope (FESEM) for the AC produced at different times on reaction. It can be clearly seen that as the duration of the activation process increases, the macrospores formation takes place and web-like structure can be seen for 30 h reaction time. This contributes to achieve an enhanced electrochemical performance [130]. The results of the electrochemical performance of the material HFPC-30 with the high surface area of 1060 m^2/g and specific capacitance of 600 F/g at 1 A/g current density: a very energy density of 25.3 Wh/kg at a power density of 4320 W/kg with 85% capacitance retention after 10,000 cycles was achieved.

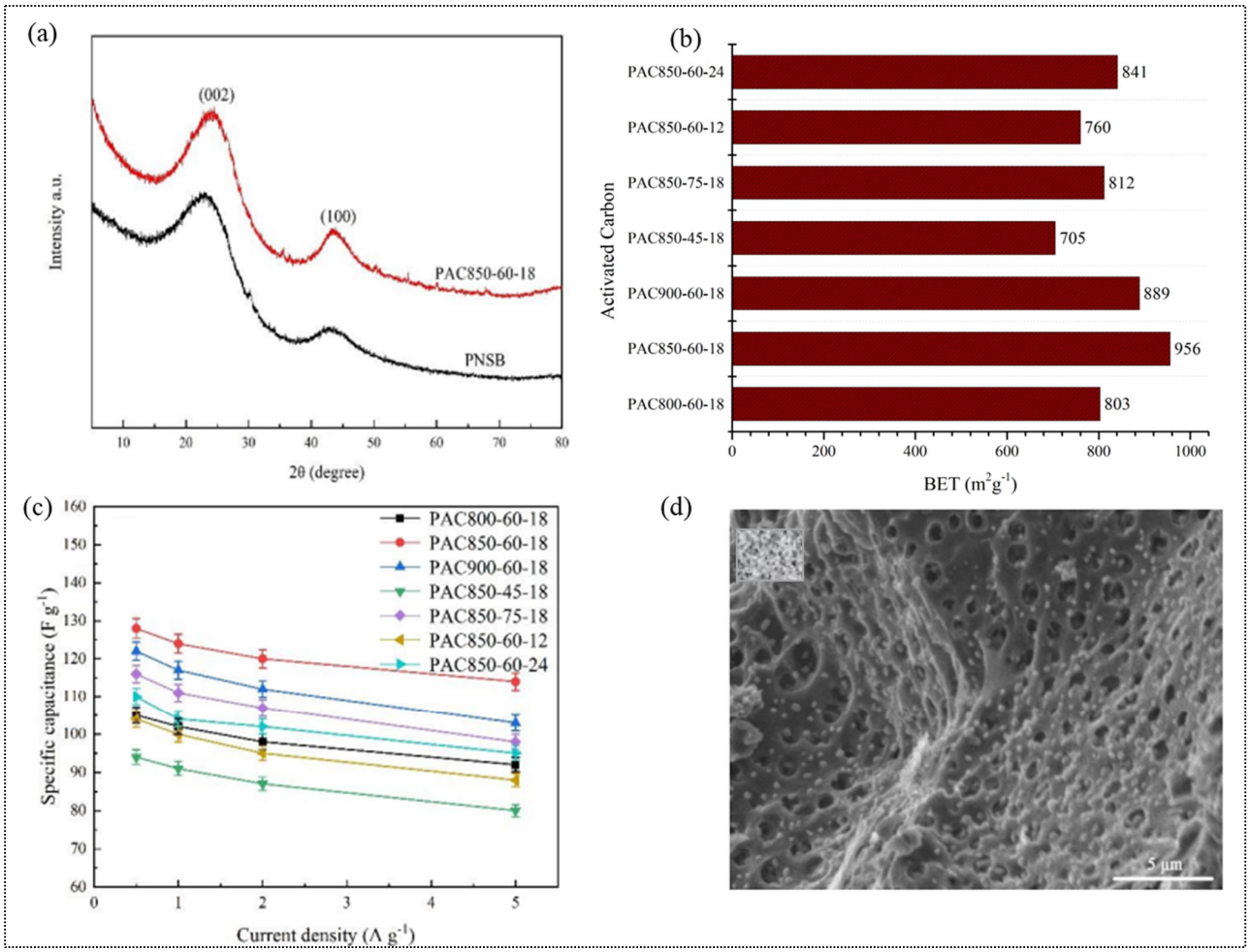

Figure 5. Physical activation of pine nut shell biochar using steam as an activating agent (**a**) XRD pattern. (**b**) BET analysis; (**c**) specific capacitance; (**d**) SEM micrograph. Reprinted with permission from Ref. [70]. Copyright 2019 ESG Publishing.

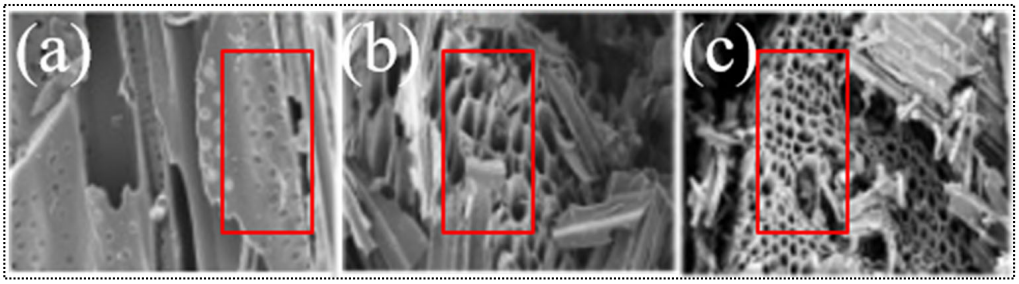

Figure 6. FESEM images: (**a**) HFPC-10, (**b**) HFPC-20, and (**c**) HFPC-30. Reprinted with the permission from Ref. [130]. Copyright © 2022 Elsevier B.V.

3.1.2. Chemical Activation of BC

Chemical activation of the BC has two major steps, which constitute of the activator mix and calcination at elevated temperatures. Generally, the biomass that needs to be thermally treated undergoes mixing with the activating agent at an optimized ratio and is then activated at an elevated temperature in order to have suitable results. Activating agents may be bases, acids, and slats. These can be impregnated into the desired materials with the help of physical mixing and stirring [131]. Activating conditions, precursors, and the structure of the activated material play a vital part in assessing the electrochemical performance of the produced material. In some cases, biomass-derived BC is produced via

pyrolysis and the impregnated char is then heated in a nitrogenous environment to make activated carbon; chestnut derived-BC is produced and activated by the post-treatment method to make activated carbon as a promising electrode material for energy storage [76]. Surface-modified AC was obtained from corncob biomass precursor; hydro-char was post-treated with $ZnCl_2$, H_3PO_4, and KOH followed by activation at 600 °C. It was observed that KOH-activated BC executed the highest surface area among all tested materials–up to 1222 m^2/g [132]. Pretreatment of biomass precursor with an activating agent and then subjecting the pretreated material to pyrolysis is another way to produce AC; oil palm shell impregnated with $ZnCL_2$ was subjected to pyrolysis at different temperatures to achieve AC [133].

In the chemical activation method, the activator has a prime role to affect the properties of activated BC; among these, KOH has special benefits to achieve high yield with controlled pore features of microporess, mesopores, and a high specific surface area at lower temperatures [134]. KOH activation is generally employed by the help of a two-stage process (pre-heat treatment and subsequent activation). A range of biomass has been employed for the production of BC, which is further activated by KOH and NaOH as activating agents. These materials were employed for the application of supercapacitors. The physical attributes of porosity can be elaborated by the help of subsequent multiple steps. In the beginning, these oxidants oxidize the carbon into carbonate ions. Post-washing of metal compounds also develops further pores. Then, M_2CO_3 decomposes into CO or CO_2, leading to further pore development. The general reaction scheme for chemical activation by alkali is as follows shown by Equations (4)–(7), where M denotes the alkali metals like K or Na [135].

$$2MOH + CO_2 \rightarrow M_2CO_3 + H_2O \uparrow \quad (4)$$

$$2C + 2MOH \rightarrow 2CO \uparrow + 2M \uparrow + H_2 \quad (5)$$

$$M_2CO_3 + C \rightarrow M_2O + 2CO \uparrow \quad (6)$$

$$M_2O + C \rightarrow 2M \uparrow + CO \uparrow \quad (7)$$

Zhang et al. [136] evaluated the impact of KOH dosage and various values of the activating temperature to produce BC from Xanthoceras sorbifolia seed coats. His findings were are follows: an increase in KOH dosage and a rise in activation temperature caused an increase in surface area of 2445 m^2/g and specific capacitance of 423 F/g [136]. For example, activated porous carbon from bamboo via carbonization followed by activation showed 293 F/g capacitance at $0.5Ag^{-1}$ [137]. Figure 7 shows MnO_2 loaded crosslinked carbon nano sheet (MnO_2@CCNs) preparation via KOH activation. These metal oxide loaded sheets can be made in two ways; one is pre-treatment with KOH, and the other is post-treatment followed by hydrothermal deposition of metal oxides [138].

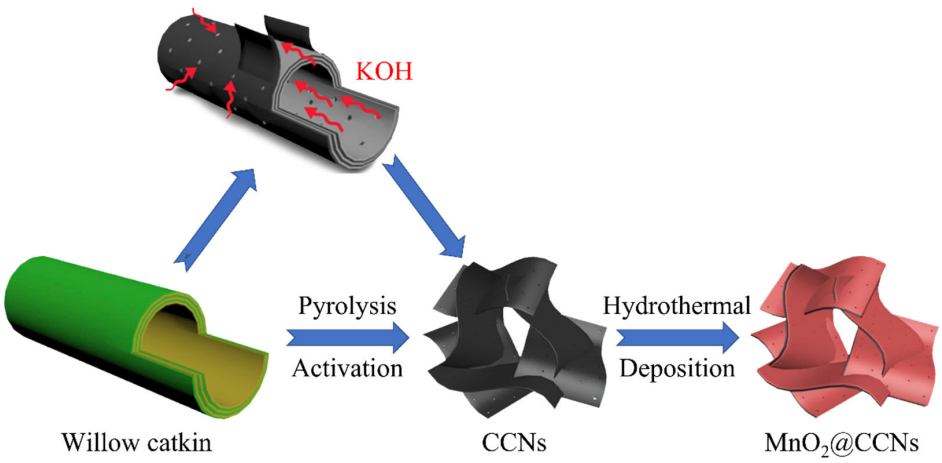

Figure 7. Preparation scheme of manganese oxide loaded carbon nano-sheets by KOH activation supercapacitors. Reprinted with permission from Ref. [138]. Copyright © 2015 Elsevier B.V.

The pyrolysis of rice straw followed by KOH activation was carried out to synthesize AC. This AC showed promising electrochemical performance by exhibiting a capacitance of 332 F/g for supercapacitor applications [139]. One-step KOH activation is also being widely used to produce AC for energy storage. Pyrolysis of corn husk treated with KOH was carried out to produce porous carbon, which showed an excellent capacitance of 356 F/g [68]. Recently, hierarchically porous carbon material synthesis was reported using $KHCO_3$ as an activator [19,140]. Chestnut seed precursor was used to make AC by physical and chemical activation methods, coupled with pyrolysis. Figure 8a presents the morphology of BC before activation and the formation of large pores with a low specific surface area of 17.1 m^2/g, while a noticeable change in structure and specific surface area occurs after activation [76]. While Figure 8b shows that during physical activation with CO_2, the specific surface area increases up to 105.7 m^2/g with smaller pores, while in the chemical activation method in Figure 8c, there is a significant change in structure with various micropores that have a high specific surface area of 1221.2 m^2/g [76]. Figure 8d,e depicts the electrochemical analysis. Cyclic voltammetry curves of non-activated carbon, and physically and chemically AC were recorded at 10 mVs^{-1} and 100 mVs^{-1}. Due to the activation process, an increase in surface area leads to a higher value of capacitance. There is a promising increase in the case of chemical activation, which is due to the formation of micropores that causes the well confinement of ions.

A higher carbon yield, developed and larger porosity, and lower pyrolysis temperature are some of the advantages of chemical over physical activation. These factors are of great importance to store energy in supercapacitors [141].

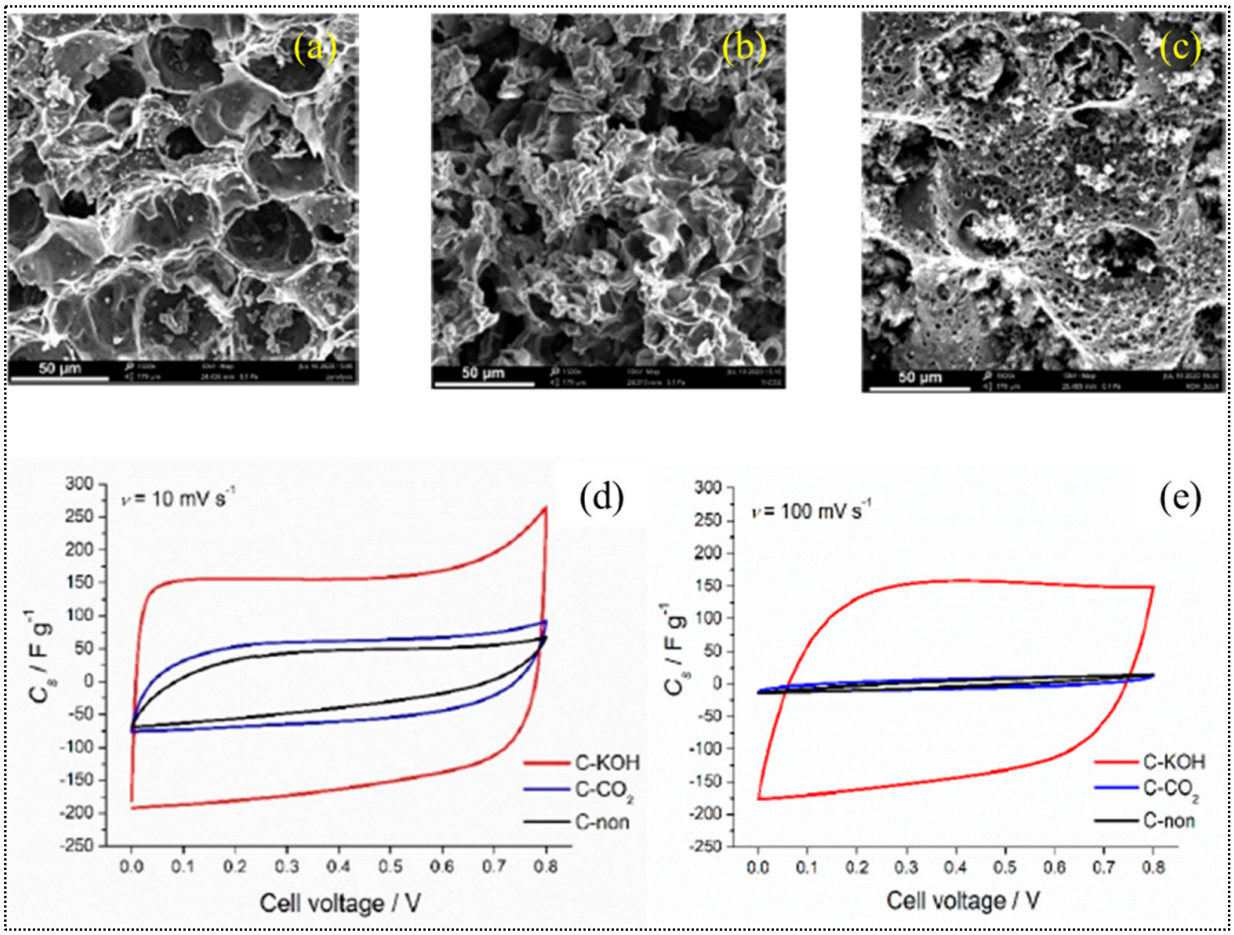

Figure 8. SEM Images of: (**a**) non activated, (**b**) physical activated carbon, (**c**) chemically activated carbon, (**d**) cyclic voltammetry curves at 10 mVs^{-1} (**e**) at 100 mVs^{-1}. Reprinted with permission from Ref. [76]. Copyright © 2020 MDPI.

It has been previously reported that potato starch-derived AC was produced using KOH activation for supercapacitor applications. An increasing ratio of KOH/AC and decreasing carbonization temperature resulted in achieving a 335 Fg^{-1} capacitance with increased SA [142]. In the same way as the different ratios of KOH to BC, activated BC was derived from bamboo, which showed the development of micropores is nearly completed at a ratio of BC/KOH = $\frac{1}{2}$, while increasing the ratio of BC/KOH to 1/3 leads to an increased mesoporous fraction, which is due to larger pores. When the ratio is increased to $\frac{1}{4}$, the surface area reaches from 1010.21 to 1413.21 m^2/g. Similarly, the total pore volume is affected by the increasing ratio, which increases from 0.123 to 0.708 cm^3/g. It was also concluded that a higher mesoporous fraction showed a higher capacitance due to an effective mobility of ions from larger pores [143]. AC derived from corncobs via chemical activation was used as an electrode material for supercapacitors, which achieved 401.6 F/g high specific capacitance in 0.5 M H_2SO_4 and 328.4 Fg^{-1} in 6 molar KOH electrolytes at 0.5 Ag^{-1} current density. The highest specific surface area of 3054 m^2/g with favorable functional groups and well developed micro porosity and electronic conductivity was exhibited by the AC synthesized at a temperature of 850 °C [144]. The direct KOH activation method was applied to synthesize AC from miscanthus grass, which was investigated at different reaction times for 6, 12, 18, 24, and 48 h and with chemical pretreatment of biomass in an aqueous solution of KOH 16% (*w/v*) under stirring at 25 °C. At a current density of 0.5 A/g, a specific capacitance of 162 F/g was exhibited by miscanthus-derived AC synthesized after 18 h pretreatment with KOH and a micropore volume of 0.26 cm^3/g and surface area of 639 m^2/g. In the case of 12 h pretreatment with KOH, AC showed an energy density of up 14.4 Wh/kg and current density up 377 W/kg with stable performance [15].

Chemical activation is the most common and effective process to produce surface modified AC with a well decorated porosity and high surface area. However, expensive chemicals, post washing of these chemicals, and unwanted hazardous by-products are the challenges associated with this process of activation.

3.1.3. Physiochemical Activation of BC

The physicochemical activation method is a technique to activate the BC by the combination of both physical and chemical methods [145]; an activating agent is used to treat the precursor feedstocks or char, followed by pyrolysis in the reactor in an oxidant flow to make activated material [146]. This method is utilized when it is difficult to remove the activating agent used in the activation process through washing; otherwise, it can cause blockage of pores. [147]. High temperature, long process time, and lower yield are some of the issues associated with this method.

Thus Hu et al. [148] studied the combined effect of this method of activation to achieve high mesoporosity by applying CO_2 activation at 800 °C to KOH or $ZnCl_2$ AC produced from coconut shell and palm stone. His findings were of an increased surface area up to 2400 m^2/g and mesoporosity from 14–94%. Previously, AC produced from coffee grounds via physical, chemical, and a combination of both methods was studied. The results revealed a 405.68 m^2g^{-1} high surface area in the case of chemical activation, followed by the combination of physical and chemical activation at 133.72 m^2/g, and 35.45 m^2/g for physical activation [149]. E. Taer et al. [74] used sugarcane bagasse precursor to make AC by physical process and physicochemical process. SEM micrographs in Figure 9 clearly shows that AC produced via the physicochemical method is more porous than AC produced by the physical activation process. The specific capacitance achieved by physical AC was 146 F/g, while in case of physicochemical AC it increased to 176 F/g. Physiochemical activation has been less studied to synthesize AC for supercapacitor application because it involves two activation processes.

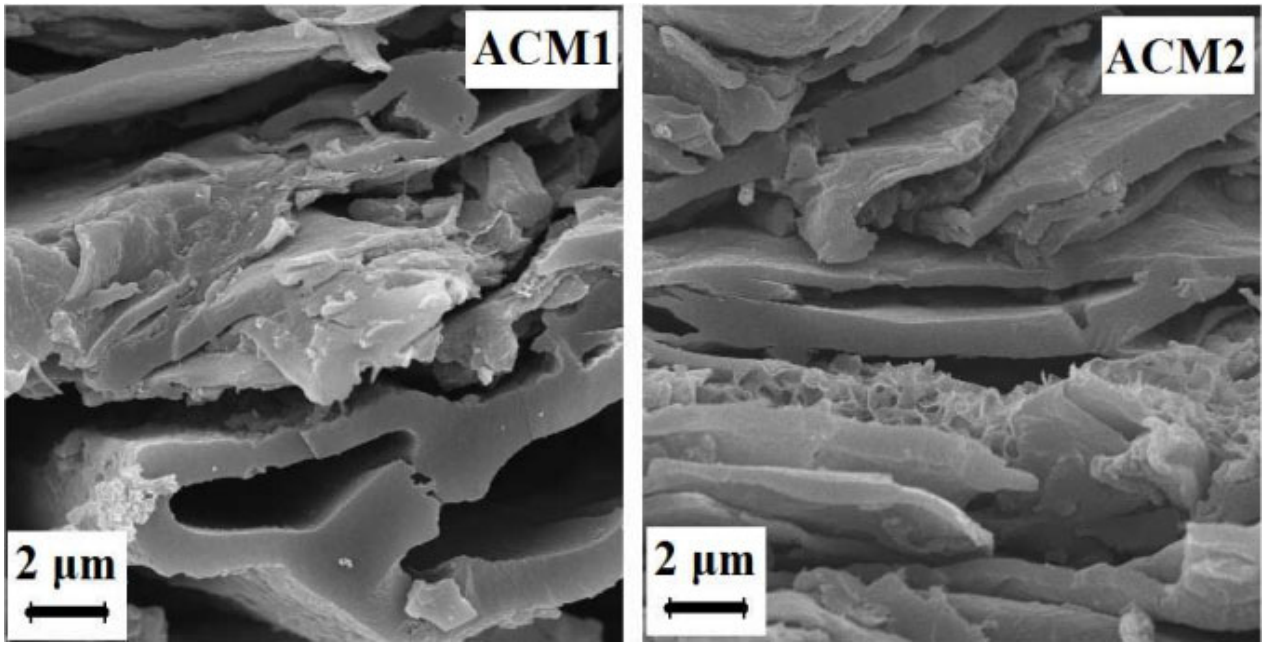

Figure 9. SEM micrographs. ACM1 activated carbon via physical activation, and ACM2 activated carbon via physicochemical activation. Reprinted with permission from Ref. [74]. Copyright © 2022 by Trans Tech Publications Ltd.

Activation methods including physical, chemical, and physicochemical activation are used to produce AC for different applications such as energy storage. These methods have some advantages and disadvantages, which are summarized in the Table 2.

Physiochemical activation implemented to synthesize activated carbon for supercapacitor applications has been less studied because it involves two activation processes. Table 3 summarizes the physical, chemical, and jointly physiochemical activation methods used to produce activated BC-based materials from different biomass feedstocks. The electrochemical performance of activated carbon produced via different activation techniques for supercapacitors has been discussed.

Table 2. Advantages and disadvantages of activation techniques.

Activation Method	Advantages	Disadvantages
Physical activation	Commercial scale application, easy adoptability, biochar with enhanced porosity and physical strength	Lower yield of biochar, longer activation time, high activation temperature, high energy consumption
Chemical activation	Higher biochar yield, high surface area, developed and larger porosity and lower activation temperature	Expensive chemicals, post-washing of these chemicals, unwanted hazardous by-products
Physicochemical activation	It is utilized when it is difficult to remove the activating agent used in activation process through washing	Less studied method of activation, lower char yield, high temperature

Table 3. Activated carbon production from different biomass feedstocks via activation methods and application for supercapacitor electrodes. Adapted with permission from Ref. [150].

Lignocellulosic Biomass	Activation Methods	Specific Surface Area (m^2/g)	Current Density (Ag^{-1})	Specific Capacitance (Fg^{-1})	Electrolyte	Energy Density (Wh/kg)	Power Density (W/kg)	Ref.
Rice husks and crab shells	Chemical activation by KOH	3557	0.5	474	6 M KOH	—	—	[151]
Corn husk	Activation with KOH	1370	1	127 and 80	6 M KOH and 1 M TEABF4/AN	20	681	[152]
Sisal	KOH activation	2289	0.5	415	6 M KOH	—-	—-	[153]
Camellia oleifera shell	Chemical activation with $ZnCl_2$	1935	0.2	374 and 266	1 M H_2SO_4 and 6 M KOH	—-	—-	[154]
Rose flower	Chemical activation with KOH/KNO_3	1980	1	350	6 M KOH	—-	—-	[155]
Sunflower seed shell	KOH activation	1162	0.25	244	30 wt% KOH	4.8	2.4	[156]
Rice husk	Carbonization at 450 °C and chemical activation by KOH at 400–900 °C	3145	2.27	367 for aqueous electrolyte and 174 for organic electrolyte	6 M KOH	—-	—-	[157]
Rice husk	Carbonization at 400 °C in muffle furnace of NaOH pretreated rice husk, activation by KOH at 750 °C, 850 °C, and 950 °C	2696 at 850 °C	0.1	147 at 850 °C	6 M KOH	5.11	—-	[158]
Poplar anthers	Chemical activation with KOH	3639	0.5	361.5	6 M KOH			[159]
Apricot shell	NaOH activation	2335	0.5	339	6 M KOH	—-	—-	[160]
Rice husk	Chemical activation with KOH	3263	0.5	315	6 M KOH			[161]
Castor shell	Chemical activation with KOH	1527	1	365	6 M KOH	—-	—-	[162]
Cornstalk	Chemical activation with $K_2C_2O_4 \cdot H_2O$	2054	0.5	461	1M Na_2SO_4	—-	—-	[163]
Husk of cotton Seed	Chemical activation with KOH	1694.1	0.5	1694.1	6 M KOH	—-	—-	[164]
Cotton stalk	Chemical activation with KOH	1964.46	0.2	254	1 M Na_2SO_4	—-	—-	[165]
Waste tea leaves	Chemical activation with KOH	2841	1	330	2 M KOH	—-	—-	[166]
Corn grains	Chemical activation with KOH	3199	0.5	257	6 M KOH	—-	—-	[167]
Mantis shrimp shell	Self-activation at 700 °C, 750 °C, 800 °C, 850 °C, and 900 °C with N-S co-doping	401	1	201	6 M KOH	—-	—-	[25]
Grape Marcs	Doping with N and CA with KOH at 700 °C	2221.4	0.5	446	1M H_2SO_4	16.3	348.3	[150]
Quinoa	N doping with CA with different KOH ratios.	2597	0.5	330	6 M KOH	9.5 in aqueous electrolyte and 22 in organic electrolyte	—-	[168]

3.2. Metal Oxide Loaded Modified BC for Supercapacitors

Surface loading with metal/hydroxides is another way to change the surface of the BC. Metal loading is a process in which the BC surface is loaded with the transition metal oxides to change its features. BC acts as a substrate to support the metal oxides and hydroxides to increase surface redox activity. Among all metal loading methods, the most common and developed method is impregnation. By this method, the metallic particles are impregnated into the pores of the BC by capillary action [169,170]. To make a compatible BC-based material with transition metals oxide, two activation techniques are used: the first is acid activation and the second is alkali activation–the alkali activation mechanism. Raw algal biochar (RAB) was prepared via pyrolysis at a heating rate of 15 °C/min reaching the reaction temperature of 700 °C. RAB is the precursor to synthesize 3D interconnected mesopores network (3DFAB). Green microalgae was treated with 6 M NaOH and refluxed for 5 h at 100 °C. 3DFAB synthesized by pyrolysis at 700 °C for 2 h followed by reflux by H_2SO_4 and HNO_3 for 6 h at 80 °C [171].

Figure 10 presents the mechanism of alkali activation. In this method, the BC sample is mixed with an activating agent followed by thermochemical conversion. During pyrolysis, the reaction of NaOH with carboxyl, carbonyl, hydroxyl, ether, and ester groups takes place. As a result, free radicals and vacancies are generated. Other reactions of NaOH with C-C and C-H also generate vacancies. The formation of many oxygen functional groups takes place due to the penetration of OH and NaOH into vacancies [171]. The impregnation of metallic particles becomes easy because the metal uptake is enhanced due to acidic functional groups, which are obtained during chemical treatment by acid while contact between metal and carbon increases with basic treatment [172–174]. Oxides or hydroxides MnO_2, NiO, Co_3O_4, Ni $(OH)_2$, and $Co(OH)_2$ of transition metals are reported as pseudo-capacitor materials [175]. However, metal oxides/hydroxide loaded BC-based materials act both as a pseudo-capacitor and electric double layer capacitor. Previously, it was studied that BC obtained from wood used a substrate to grow MnO_2. The redox reaction of BC and $KMnO_4$ makes BC loaded with manganese oxide [19].

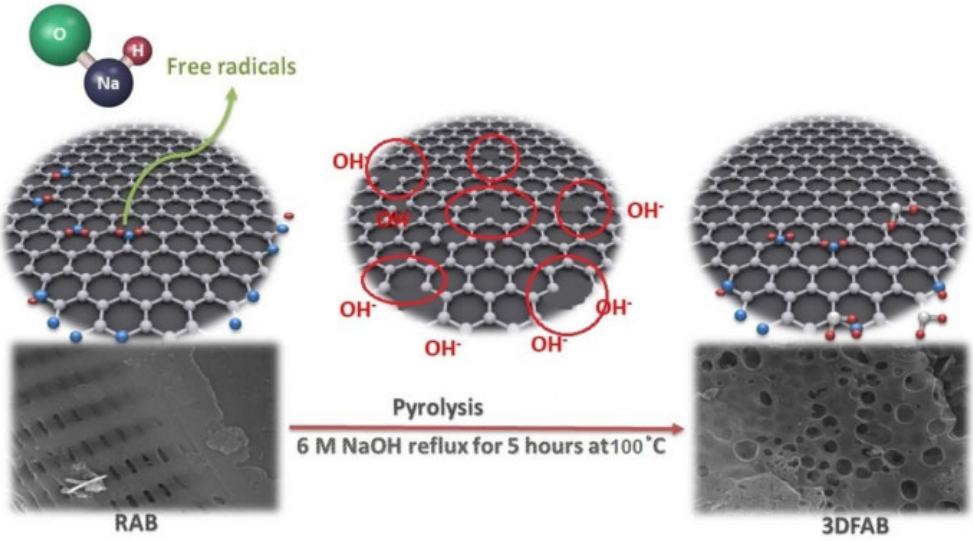

Figure 10. Alkali activation mechanism prior to synthesize metal oxide-loaded BC. Reprinted with permission from Ref. [171]. Copyright © 2021 Springer Nature.

Banana stem-derived BC was obtained via pyrolysis at 500 °C for 12 h. Iron oxide-loaded magnetic BC was made by treating raw BC with $FeCl_3$ and $FeSO_4$ solutions. The surface area increased from 7.97 m^2g^{-1} to 283 m^2g^{-1}, which happens due to the fusion of metallic particles on the surface of the BC. To enhance the conductivity and capacitance, the magnetic BC was transformed to a composite with conducting polymer polyaniline. The

magnetic BC and composite demonstrated specific capacitances of 234 F/g and 315 F/g, respectively [176].

Metal oxide-loaded BC-based materials exhibited excellent electrochemical performance for supercapacitors. However, it is still a challenge to control the doping content of metal oxide. BC based as a career for this method should be optimized in its structure and porosity.

3.3. Heteroatoms Doped BC for Supercapacitors

The low manufacturing cost, low toxicity, high cycle stability, and environmentally friendly nature of the AC make it a promising candidate for the construction of electrodes for supercapacitors. [177,178]. The electrochemical performance of storage devices can be enhanced by enhancing the surface area, conductivity for current, and stable structure of the electrodes [179,180]. Doping BC with heteroatoms is an alternative way to change the surface features of BC to improve its electrochemical performance. Doping of nonmetals like nitrogen, sulphur, phosphorous, boron, fluorine, and metallic atoms like gold, silver, cobalt, and iron has received attention with regard to the modification the carbon-based materials. The atomic size and electronegativity of the nonmetal dopants can effectively enhance the charge storage capacity of the devices [181–183]. The main atoms to be used for surface doping are S, P, N, O, and B. To improve the performance of BC, a single atom doping of N is most commonly used. N-doped BC can be produced via two routes; one is N self-doping, which is conducted with biomass that contains N containing components. Figure 11 shows the scheme to fabricate N-doped BC for supercapacitor applications. It is implemented in two steps: carbonization, followed by pyrolysis. These nitrogen-containing precursors can be converted into N-doped BC via in-situ pyrolysis as also discussed by [184,185], while in the second route, one N-doped BC can be obtained by nitrogen-containing dopants like urea, thiourea, NH_4Cl, etc. These elements can be co-doped with two or more in number on BC-based materials. This modification technique can control the electronic properties of BC-based materials, while improving the conductivity and wettability, whilst the additional reaction of functional groups may occur to produce pseudo-capacitance [186–188]. Biomass originates from plants and animals that are usually rich in carbon, but contains also other nonmetal atoms that are uniformly distributed; due to this modification method, doped BC-based materials can easily be made via simple annealing [189–191]. Previously ultrathin graphitic carbon was produced via KOH activation from green tea waste biomass, which exhibited a good specific capacitance and excellent cycle stability [192].

To tune the surface of BC, this doping is an alternative approach to modify the surface of BC-based materials to improve the capacitance performance. N-rich hierarchical carbon electrode with a 2221.4 m^2g^{-1} high surface area prepared from grape marcs exhibited an excellent charge storage ability in electrolyte of 1 M H_2SO_4 at a 0.5 Ag^{-1} current, density maximum of 446.0 Fg^{-1}, and a capacitance compared to 6 M KOH and 1M Na_2SO_4 with specific capacitances of 345.5 Fg^{-1} and 310 Fg^{-1}, respectively. Supercapacitors assembled by these materials showed excellent performance by reaching 16.3 $Whkg^{-1}$ energy density with 348.3 Wkg^{-1} power density [150]. Self-activation was proposed to make N-S co-doped hierarchical porous BC-based materials from mantis shrimp shells using pyrolysis at different temperatures of 700 °C, 750 °C, 800 °C, 850 °C, and 900 °C for supercapacitors. Electrochemical tests revealed that at an activation temperature of 750 °C BC achieved 401 $m^2g^{-}1$ SA, a 1 Ag^{-1} current density, a highest specific capacitance of 201 Fg^{-1}, and nitrogen contents (8.2 wt%) and sulfur contents (1.16 wt%) in 6 M KOH electrolyte [193].

Doping of biochar with heteroatoms-based materials demonstrated excellent performance for supercapacitors, however, the effect and mechanism of heteroatoms doping towards electrochemical performance is still not clear. The working mechanism of different types of heteroatoms doping is unclear, and it is also difficult to control the concentrations and ratios of different doping species. Table 4 summarizes the metal loaded and heteroatoms doping of different biomass feedstocks for electrochemical applications.

Table 4. Modified BC-based materials via metal loaded and heteroatoms doped BC as an electrode materials for supercapacitor application. Recreated from the references [125,150].

Lignocellulosic Biomass	Modification Method for Supercapacitor Materials	Capacitance (F/g)	Current Density (F/g)	Electrolyte	Cycle Stability (%)	Ref.
Bagasse	MnO_2/Porous carbon	492.5	1	6 M KOH	92.1% after 5000 cycles	[195]
Typha domingensis	Ni–Co oxides/nanofibers composite	142	1	6 M KOH	78.4% after 5000 cycles	[196]
Hemp straw	Fe_2O_3/porous carbon nanocomposites	256	1	6 M KOH	77.71% after 5000 cycles	[197]
Houttuynia	nitrogen-doped hierarchically porous carbon	473.5	1	6 M KOH	95.74% after 10,000 cycles	[198]
Peach gum	$Ni(OH)_2$/carbon nanosheet	350	1	6 M KOH	83.9% after 5000 cycles	[104]
Datura metel seed pod	N, S codoped activated mesoporous carbon	340	1	1 M H_2SO_4	95.24% after 3000 cycles	[199]
Elaeocarpus tectorius	Phosphorus-doped porous carbon	385	0.2	1 M H_2SO_4	96% after 1000 cycles	[200]
Carboxy methyl cellulose ammonium	co-doped hierarchically porous	465	1	3 M KOH	86.3% after 10,000 cycles	[201]
Bamboo leaves	Copper oxide/cuprous oxide/hierarchical porous carbon	147	1	3 M KOH	93% after 10,000 cycles	[202]
Lotus pollen	$CuCl_2$-activated carbon	496	1	1 M Na_2SO_4	90.8% after 10,000 cycles	[203,204]
Rape pollen	Co-doping of Nitrogen and sulfur to make hierarchically porous carbon	361	1	6 M KOH	94.5% after 20,000 cycles	[205]
Ginkgo leaves	porous carbon doped with nitrogen	323.2	0.5	6 M KOH	99% after 12,000 cycles	[206]
Peanut shells	doped BC with nitrogen	447	0.2	1 M H_2SO_4	91.4% after 10,000 cycles	[207]
Bamboo	Graphene functionalized bio-carbon xerogel	189	1	6M KOH	10% after 10,000 cycles	[208]
Tofu	Fe_3C/Fe_3O_4 nanosheets	315	0.5	6 M KOH	–	[209]
Banana peel	MnO_2 and biomass-derived 3D porous carbon composites	170	10	1 M Na_2SO_4	98% after 3000 cycles	[106]
Cotton Seed Husk	3D Porous Carbon like Honeycomb	238	0.5	6 M KOH	91% after 5000 cycles	[164]
Puffball spores	Self-doped hollow-sphere porous carbon doped with N & S	285	0.5	2 M KOH	80.3% after 5000 cycles	[210]
Paper towel	Bifunctional 3D n-doped carbon materials	379.5	1	6 M KOH	94.5% after 10,000 cycles	[211]
Potato waste	N-doped carbon activated $ZnCl_2$ and melamine	255	0.5	2 M KOH	93.7 after 5000 cycles	[212]
Pine nut shells	N-doped BC with KOH and melamine activation	324	0.5	6 M KOH	—-	[213]
Bamboo shoot Shells	N, S-doped BC	302.5	0.5	1 M H_2SO_4	—-	[82]
Bamboo	KOH activated, and HA-doped BC with N, B	281	0.2	1 M KOH	——	[214]
Peanut meal	Carbonization, $ZnCl_2$ and $Mg(NO_3)_2{\cdot}6H_2O$ activation	525	1	1 M H_2SO_4	—-	[215]

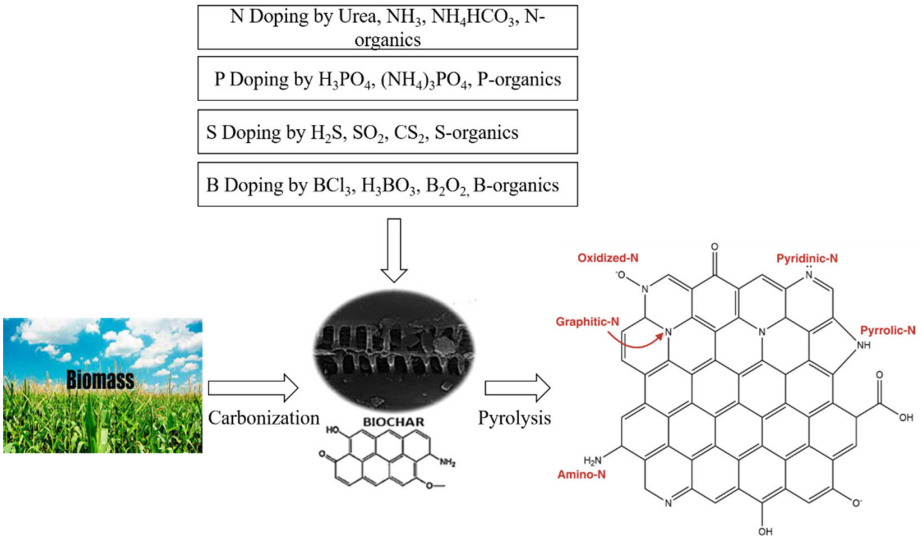

Figure 11. Scheme to make heteroatoms doped BC. Doped BC obtained by two steps; carbonization followed by pyrolysis in an inert atmosphere. Recreated with permission from Ref. [194]. Copyright © 2020 Elsevier B.V.

3.4. Modification of BC Using Sono-Chemical Method for Supercapacitors

Biomass valorization can be carried out in a variety of ways, such as microwave, gamma rays, electron beam, pulse electric field, and ultrasound technology. Ultrasonic irradiation gained attention due to its mechano-acoustic (physical) and sono-chemical (chemical) effects. The mechanoacoustic effect physically disrupts the surface of biomass, while in case of the sono-chemical phenomenon, extreme temperature and pressure due to cavitation leads to the generation of highly reactive radicals [216]. Sound waves that are higher than 20,000 Hz in frequency are categorized as ultrasound. When they transmit in a system, there would be many effects that can affect processes such as heating, mechanical, chemical, and sound effects. Solid and liquid reactions are improved by this treatment, which is due to the uniform mixing of reactants [217,218].

Figure 12 shows the schematic of the formation of porous carbon via sono-chemical modification [219]. In Figure 12 it is shown that during ultrasonic treatment, dissolved NaOH can easily penetrate into the micropores of the carbonized biomass precursor. With the increasing temperature, NaOH reacts efficiently with carbon to produce more mesopores and micropores to make porous carbons with a high surface area. Figure 13a–d displays the electrochemical performance of sono-chemically modified BC from rice straw at a relatively low activation temperature. At a temperature of 600 °C and 1 h sonication, porous carbon was produced that exhibited a 420 Fg^{-1} higher capacitance at 1.0 Ag^{-1} density. This modified BC achieved a 1820.2 m^2g^{-1} surface area with a superior rate performance of 314 Fg^{-1} at 10 Ag^{-1}. The supercapacitor showed a high electrochemical performance by achieving an energy density of 11.1 Wh/kg and power density of 500 W/kg. The cycle's stability after 10,000 cycles up to 99.8% was achieved at 20 Ag^{-1} current density [219].

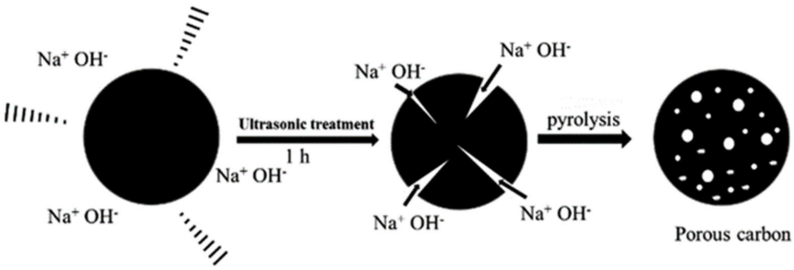

Figure 12. Representation of sono-chemical method to produce surface modified porous carbon. Reprinted with permission from Ref. [219]. Copyright © The Royal Society of Chemistry 2020.

Due to acoustic cavitation [220,221], mechanical and chemical effects produced by ultrasound can enhance the mass transfer [222,223], due to which the formation and destruction of microbubbles take place in the liquid. All these results suggested that the ultrasound-assisted method is an effective technique that can produce a stable electrode material at a lower activation temperature for supercapacitors [125]. Two routes were studied to modify the surface of the char produced from coconut shell using hydrogen peroxide as an oxidizing agent. In the first route, char was mixed with H_2O_2 and then activated with KOH; in the second route, char mixed with H_2O_2 was sonicated and then activated with KOH. Results showed that a maximum specific surface area of 2700 m^2/g achieved at 30% concentration of H_2O_2 assisted with sonication, while ultra-sonicated activated char exhibited high a specific capacitance of 487 F/g, and char without sonication achieved 296 F/g [224]. Bean dregs biomass derived porous carbon obtained via ultrasonic activation coupled with KOH treatment showed a high specific surface area of 1281 m^2/g and specific capacitance of 197 F/g [225]. Recently, it was studied that ultrasonic activation can reduce or clean the ash of BC to make more pores, due to which the specific surface area is increased [226]. From all of the above studies, it can be concluded that sono-chemical treatment improves the electrochemical performance of AC derived from biomass.

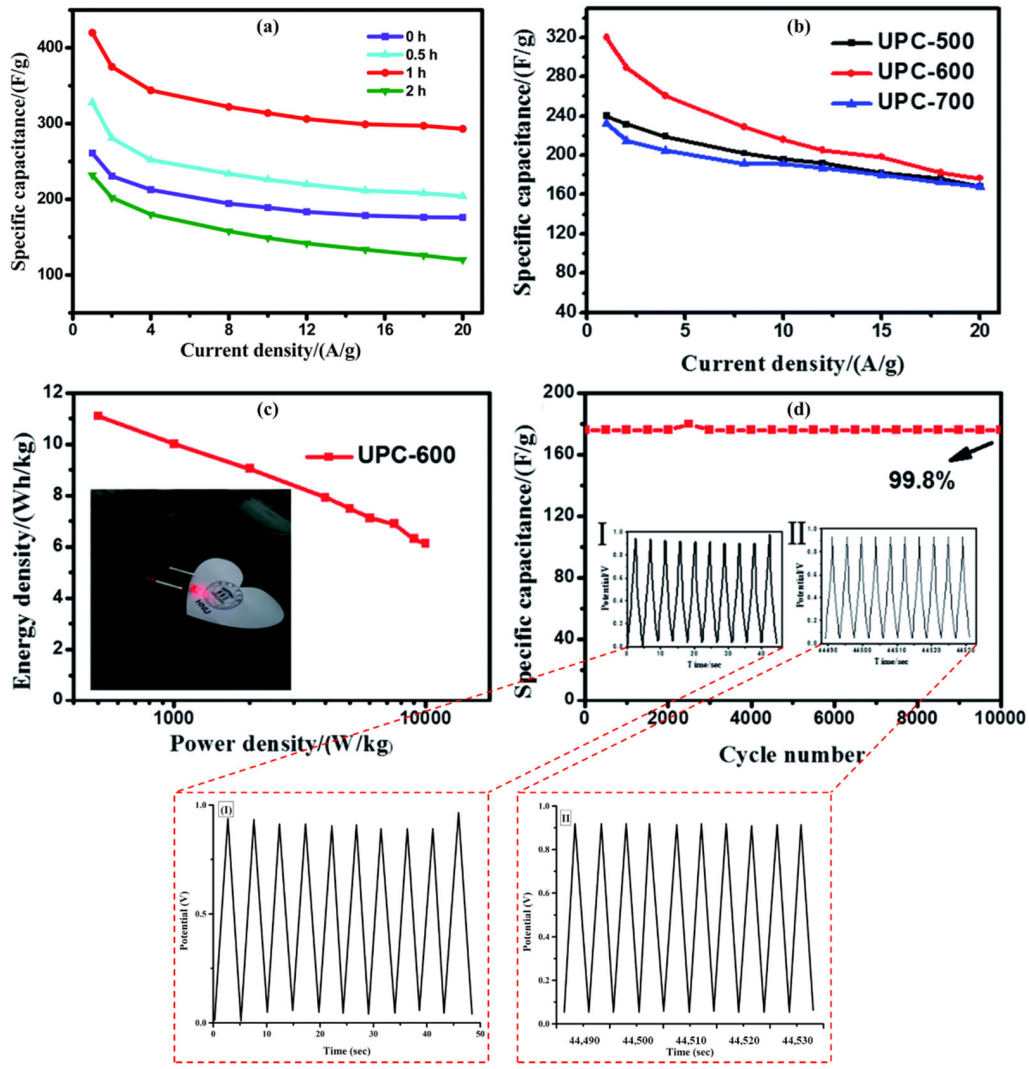

Figure 13. (**a**) Specific capacitance at current density (**b**) Specific capacitance at temperatures 500, 600 and 700 °C (**c**) Energy and power densities (**d**) 99.8% cyclic performance for 10,000 cycle numbers loaded at 20 A/g. The inset figure is the first 10 (**I**) and the last 10 times (**II**). Reprinted with permission from Ref. [219]. Copyright © (2020) The Royal Society of Chemistry.

This technique has many advantages for biomass pretreatment and the conversion of lignocellulosic biomass to valuable products like modified BC-based materials. However, there are many issues that need to be addressed. The challenge is to scale it up from the laboratory scale to the industrial scale. Furthermore, the effects of the ultrasound method varied from biomass feedstocks and processes. These can be studied by comprehensive models that can predict the viability of ultrasound-assisted processes.

3.5. Modification of BC Using Mechano-Chemical Method for Supercapacitors

Mechano-chemistry utilizes the mechanical energy to change the structure and physiochemical properties of solid matter. SL James et al. [227] reported a mechano-chemical reaction–a chemical reaction initiated by absorbing mechanical energy. Lignin, cellulose, and hemicellulose are the main components of lignocellulosic biomass, which make its complex structure. This rigid structure of biomass can be destroyed by mechanical forces such as friction, compression, shear, and impact by milling treatment. After milling treatment, hemicellulose, cellulose, and lignin are more accessible to catalysts or enzymes. Biomass is a sustainable precursor for BC-based materials synthesis [19]. There are many applications where BC-based materials can be used widely; these are energy storage, catalysts, adsorption, etc. There are many techniques for BC preparation, such as pyrolysis, hydrothermal carbonization, ionothermal carbonization, torrefaction, etc. [228,229]. Previously, it was studied that the blending and torrefaction of biomass feedstocks can play a vital role in carbon enrichment [230]. Figure 14 presents the BC-based materials can be made by coupling the abovementioned techniques with mechano-chemical synthesis. The ball milling technique can be used as an individual, or it can be coupled with some other methods to destroy the building blocks of the precursors or BC [26]. To enhance the biomass valorization, there can be changes in the structure of biomass due to mechanical pretreatment along with some other pretreatments: surface area [231,232], particle size [233], degree of polymerization [234], crystallinity index of cellulose [233,235], and thermal stability [236].

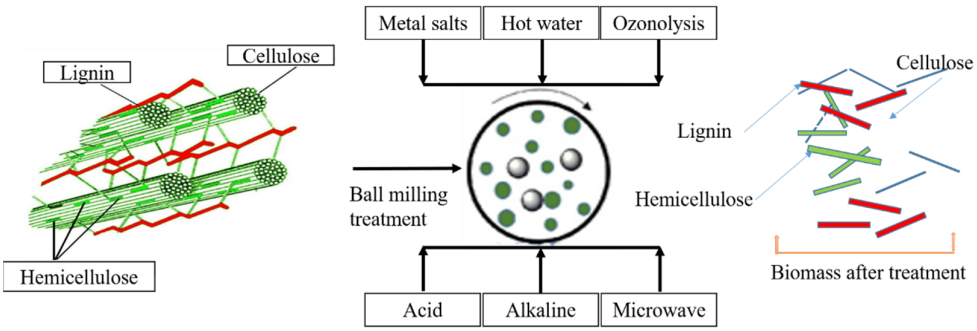

Figure 14. BM method coupled with other techniques to destroy the complex structure of lignocellulosic biomass. Recreated with permission from Ref. [26]. Copyrights © 2020 Elsevier B.V.

Xidong Lin et al. [237] proposed a green and an activation-free method to prepare BC-based materials from agro-residues through mechano-chemistry. The BC-based material was obtained by ball milling treatment, followed by carbonization with a high surface area of 1771 m^2/g compared to direct carbonization with a lower surface area of 5 m^2/g; it also demonstrate excellent electrochemical performances. Figure 15 depicts a green, solvent-free, and top-down approach to produce high-surface-area BC-based materials from biomass precursors [237]. This is a clear depiction that mechano-chemical treatment followed by carbonization produces surface-modified BC-based material with a high surface area in comparison to simple carbonization.

Figure 16a–c demonstrates the ball milling at 350 rpm for 30 min was performed, followed by pyrolysis at a high temperature (>800 °C) of dairy manure and eggshell wastes. Some of the $CaCO_3$ acted as an activating agent, decomposing CO_2 in order to produce micropores, and the removal of CaO and remaining $CaCO_3$ by HCl solution produced mesopores, which led to the production of hierarchical porous carbons for making

electrodes for supercapacitors [238]. The porous carbon produced by this method achieved a maximum surface area of 543.6 m^2/g and its total pore volume was 0.48 cm^3g^{-1}. It has promising electrochemical performance due to it exhibiting a specific capacitance of 226.6 Fg^{-1}. After 2500 GCD cycles, it performed 100% capacitance retention.

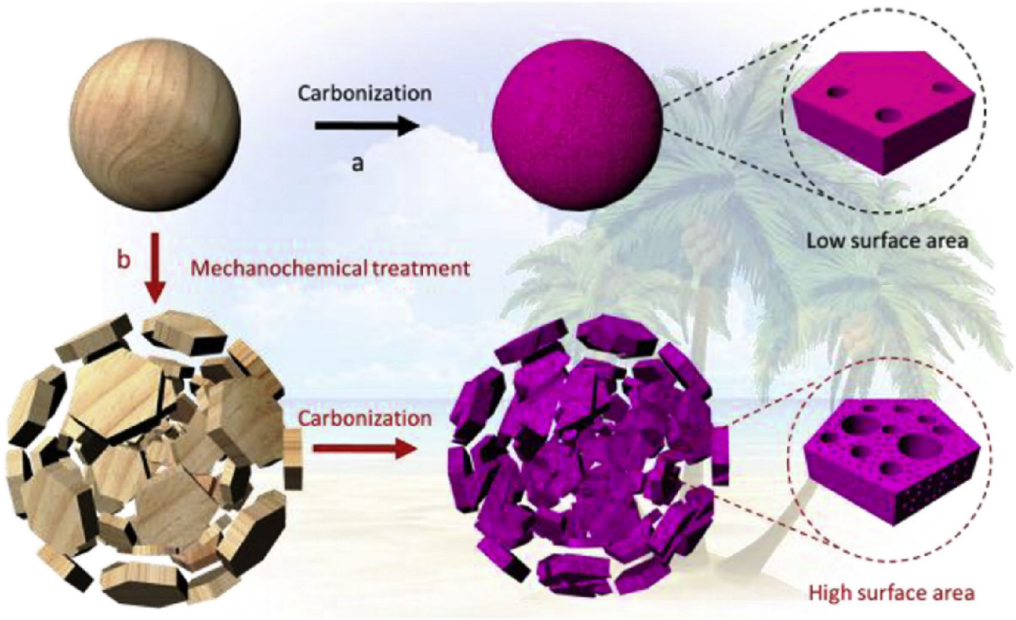

Figure 15. Comparison of surface modification of BC-based materials by carbonization and its combination with the ball milling method. Route (**a**) carbonization, Route (**b**) mechano-chemical treatment followed by carbonization. Reprinted with permission from Ref. [237]. Copyright © 2017 American Chemical Society.

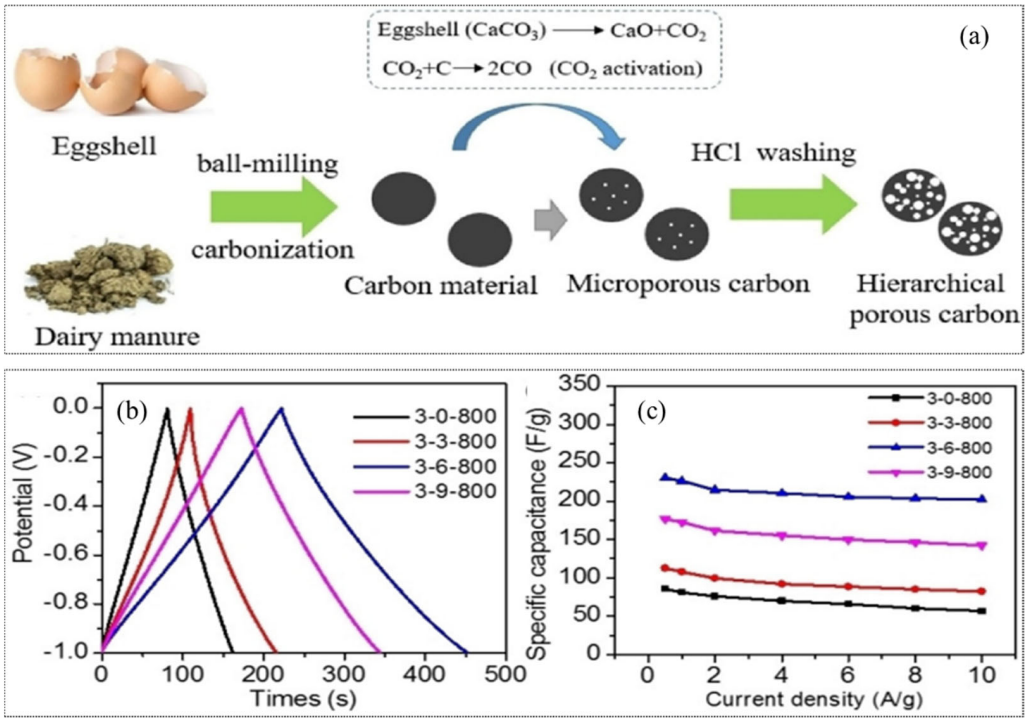

Figure 16. (**a**) Synthesis scheme of hierarchical porous carbon produced from dairy manure and eggshells via the BM technique (**b**) charge and discharge curves of samples at current density of 1 A/g (**c**) specific capacitance of samples at different current densities. Reprinted with the permis-sion from Ref. [238]. Copyright © 2018 John Wiley & Sons.

BC-based materials are sustainable and low-cost supports for metallic catalysts [239]. Generally, these metallic catalysts are fabricated by wet impregnation. Mechano-chemical is a technique that provides a green and solvent-free synthesis of electrode material and metal catalyst. Previously, two tracks were adopted via a mechano-chemical method; (1) pyrolysis of biomass followed by ball milling with oxide of iron (Fe_3O_4), and (2) biomass and metal precursor were ball milled and then pyrolyzed to produce metal-coated BC-based material [240,241]. Figure 17 presents the mechano-chemical modification provides a green route to prepare carbon/metal composite in a solvent-free environment [26].

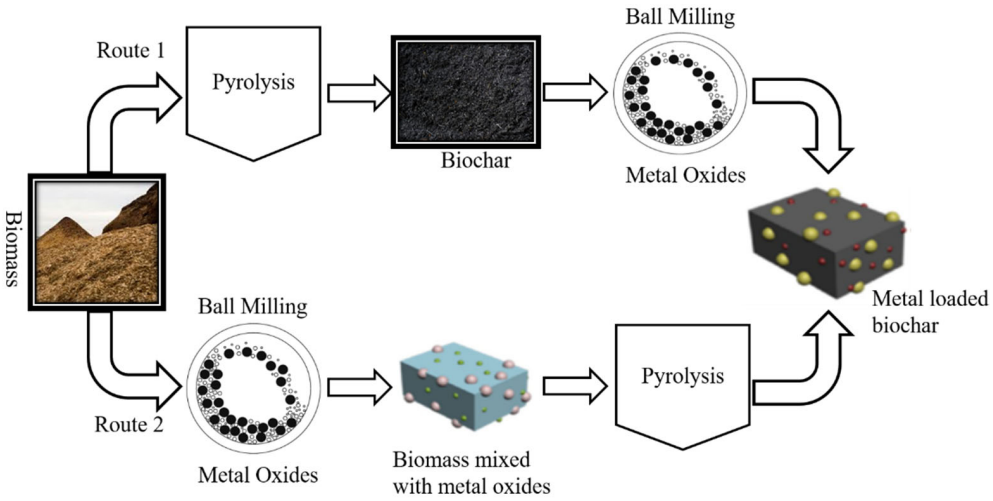

Figure 17. Two-way mechano-chemical method to produce metal oxide loaded BC-based material produced via pyrolysis. Recreated with permission from Ref. [26]. Copyrights © 2020 Elsevier B.V.

Mechano-chemical modification is a method that can be used to make nanofibers and carbon quantum dots. Surface area and oxygen-containing functional groups of BC-based materials can be enhanced by this method [242–245]. Biomass-derived porous carbon synthesized via this treatment plays multiple roles in supercapacitor applications due to its inherent heteroatoms present in the precursor biomass. Mechano-chemically modified BC-based material derived from lotus root showed a higher specific capacitance of 390 F/g due to its high specific surface area compared with chemically activated BC with a specific capacitance of 236 F/g. The energy storage device delivered the highest energy density of 9 Wh/kg at a power density of 80.8 W/kg in an aqueous electrolyte system [246]. The solvent-free approach is used to produce BC with developed micro/mesoporous structure and superhydrophilic characteristics from Corn Stover including pre-carbonization, ball milling, and activation. This method of modification enhanced the porosity, hydrophilicity, surface energy, and graphitization of the BC-based materials. Among all ball-milled activated BC at 800 °C, it presented a high specific surface area of 2440.6 m^2/g and specific capacitance of 398 F/g at 0.5 A/g the current density in 1 M H_2SO_4 electrolyte, and showed an energy density of 5 Wh/kg at a power density of 100 W/kg. XRD pattern of samples describe the crystalline structure of carbon. The broad peak centered at 22.5° was ascribed to its amorphous structure. Peak shifting at 24.5° for the ball-milled BC at 800 °C with d-spacing of 0.34 nm indicated the increased crystallinity and graphitization after milling treatment [247]. Table 5 summarizes the electrochemical performance of sono-chemically and mechano-chemically modified biochar obtained from biomass for supercapacitor.

Mechano-chemical treatment for biomass valorization has many advantages over wet processes as it does not require the consumption of any solvents and avoids post-treatment like solvent removal and product purity processing. It is being used at a laboratory scale for biomass conversion, but no data are available at the commercial level. The high energy demand to perform this method is an obstacle to its commercialization.

Table 5. Sonochemically and mechanochemically modified BC-based materials used for making electrode materials for supercapacitor applications.

Lignocellulosic Biomass	Modification Techniques	Specific Surface Area (m^2/g)	Specific Capacitance (F/g)	Current Density (A/g)	Electrolyte	Energy Density (Wh/kg)	Power Density (W/kg)	Ref.
Rice straw	Ultrasound assisted activation, which lowers activation temperature	1820.2	420	1		11.1	500	[219]
Coconut shell	Ultrasound assisted with KOH activation	2700	487 with sonication and 296 without sonication					[224]
Garlic peel	Ultrasound assisted modification	3887	426	1	6 M KOH	59.57	190.06	[248]
Lotus root	Carbonization at 700 °C for 4 h at 2 °C/min. ball milling coupled with K_2CO_3 as an activating agent in a mass ratio of 1:1 for 5 h at 500 rpm with ethanol as a reaction medium. Activation was carried out at 600 °C, 700 °C and 800 °C	Highest specific surface area of 1400 at 700 °C compared to 600 °C and 800 °C	390 with mechano-chemical modification & 236 with chemical activation	0.4	3 M KOH	9	80.8	[246]
Corn stover	Mechano-chemically BC activated at different temperatures	2440.6	398	0.5	1 M H_2SO_4	5	100	[247]

4. Knowledge Gap and Future Perspective

- Further research is requisite to understand the reactions occurring during BC production and surface modification at a macroscopic and microscopic level to be lined with biochar performance in supercapacitor applications.
- Techno-economic analysis of BC-based material production via pyrolysis and surface modification techniques is also necessary for prospects in supercapacitor applications.
- An interconnected hierarchical pore-structured BC would be a good direction to achieve the required objective. BC with improved energy storage ability and electrochemical performance need future energy storage devices.
- Efficiency comparison of different modification methods is difficult; therefore, a comprehensive comparison needs to be made at individual optimum conditions on the same BC prepared by different methods for the same energy storage application.
- More emphasized work must be conducted on the solvent-free technique mechano-chemical modification method, and also for the ultrasound-assisted method to obtain the required surface structure of BC-based materials. A combination of the ultrasound and milling effect can be more efficient to produce modified BC-based materials for energy applications.

5. Conclusive Remarks

- Physical activation is advantageous due to commercial-scale applications and adaptability. The BC materials produced by this method show the promising properties of enhanced porosity and physical strength, which are critically required to improve the electrochemical performance of supercapacitors. On the other hand, low BC yield, longer time of activation, and higher activation temperature leading to high energy consumption are issues associated with this method.

- A higher carbon yield, larger porosity, and lower pyrolysis temperature are some of the advantages of chemical activation to achieve an improved performance of supercapacitors. However, expansive chemicals and post-washing of these chemicals and by-products are some of the challenges of this method.
- Metals oxide loading on the biochar surface increases the surface redox activity. It also improves the electrical conductivity and surface area of the BC, which enhances the performance of the supercapacitor. The uniform distribution of metals is one of the challenges to be considered in this method.
- Heteroatom doping plays its role in improving the surface area, electrical conductivity, and stability of the BC for enhanced supercapacitor applications.
- Sono-chemical surface modification can modify the surface in lesser time with a lower activation temperature and improved surface area and capacitance for supercapacitors.
- Mechano-chemical modification is a solvent-free technique for surface modification of BC to achieve a high surface area, enhanced specific capacitance, and high energy density for supercapacitors. However, high energy consumption is an issue associated with this method. This technique can be coupled with various other techniques to modify the surface features of the BC for supercapacitor applications.

Author Contributions: Conceptualization, S.R.N. and A.H.K.; software, R.M.; validation, S.R.N. and R.M.; writing—original draft preparation, R.M. and A.H.K.; writing—review and editing, S.R.N.; N.A.S.A. and N.G. visualization, R.M.; supervision, S.R.N. All authors have read and agreed to the published version of the manuscript.

Funding: This research received no external funding.

Data Availability Statement: Not applicable.

Conflicts of Interest: The authors declare no conflict of interest.

References

1. Hatfield-Dodds, S.; Schandl, H.; Newth, D.; Obersteiner, M.; Cai, Y.; Baynes, T.; West, J.; Havlik, P. Assessing global resource use and greenhouse emissions to 2050, with ambitious resource efficiency and climate mitigation policies. *J. Clean. Prod.* **2017**, *144*, 403–414. [CrossRef]
2. Lee, H.W.; Kim, Y.M.; Kim, S.; Ryu, C.; Park, S.H.; Park, Y.K. Review of the use of activated biochar for energy and environmental applications. *Carbon Lett.* **2018**, *26*, 1–10.
3. Merlet, C.; Rotenberg, B.; Madden, P.A.; Taberna, P.-L.; Simon, P.; Gogotsi, Y.; Salanne, M. On the molecular origin of supercapacitance in nanoporous carbon electrodes. *Nat. Mater.* **2012**, *11*, 306–310. [CrossRef] [PubMed]
4. Qian, K.; Kumar, A.; Zhang, H.; Bellmer, D.; Huhnke, R. Recent advances in utilization of biochar. *Renew. Sustain. Energy Rev.* **2015**, *42*, 1055–1064. [CrossRef]
5. Melikoglu, M. Pumped hydroelectric energy storage: Analysing global development and assessing potential applications in Turkey based on Vision 2023 hydroelectricity wind and solar energy targets. *Renew. Sustain. Energy Rev.* **2017**, *72*, 146–153. [CrossRef]
6. Chen, Z.; Mo, F.; Wang, T.; Yang, Q.; Huang, Z.; Wang, D.; Liang, G.; Chen, A.; Li, Q.; Guo, Y.; et al. Zinc/selenium conversion battery: A system highly compatible with both organic and aqueous electrolytes. *Energy Environ. Sci.* **2021**, *14*, 2441–2450. [CrossRef]
7. Bi, Z.; Kong, Q.; Cao, Y.; Sun, G.; Su, F.; Wei, X.; Li, X.; Ahmad, A.; Xie, L.; Chen, C.-M. Biomass-derived porous carbon materials with different dimensions for supercapacitor electrodes: A review. *J. Mater. Chem. A* **2019**, *7*, 16028–16045. [CrossRef]
8. Zhang, H.; He, X.; Wei, F.; Dong, S.; Xiao, N.; Qiu, J. Moss-covered rock-like hybrid porous carbons with enhanced electrochemical properties. *ACS Sustain. Chem. Eng.* **2020**, *8*, 3065–3071. [CrossRef]
9. Wang, G.; Zhang, L.; Zhang, J. A review of electrode materials for electrochemical supercapacitors. *Chem. Soc. Rev.* **2012**, *41*, 797–828. [CrossRef]
10. Simon, P.; Gogotsi, Y. Materials for electrochemical capacitors. In *Nanoscience and Technology: A Collection of Reviews from Nature Journals*; World Scientific: Singapore, 2010; pp. 320–329.
11. Zhang, L.L.; Zhao, X.S. Carbon-based materials as supercapacitor electrodes. *Chem. Soc. Rev.* **2009**, *38*, 2520–2531. [CrossRef]
12. Matsagar, B.M.; Wu, K.C.W. Agricultural waste-derived biochar for environmental management. In *Biochar in Agriculture for Achieving Sustainable Development Goals*; Elsevier: Amsterdam, The Netherlands, 2022; pp. 3–13.
13. Sun, L.; Tian, C.; Li, M.; Meng, X.; Wang, L.; Wang, R.; Yin, J.; Fu, H. From coconut shell to porous graphene-like nanosheets for high-power supercapacitors. *J. Mater. Chem. A* **2013**, *1*, 6462–6470. [CrossRef]

14. Saikia, B.K.; Benoy, S.M.; Bora, M.; Tamuly, J.; Pandey, M.; Bhattacharya, D. A brief review on supercapacitor energy storage devices and utilization of natural carbon resources as their electrode materials. *Fuel* **2020**, *282*, 118796. [CrossRef]
15. Yakaboylu, G.A.; Jiang, C.; Yumak, T.; Zondlo, J.W.; Wang, J.; Sabolsky, E.M. Engineered hierarchical porous carbons for supercapacitor applications through chemical pretreatment and activation of biomass precursors. *Renew. Energy* **2020**, *163*, 276–287. [CrossRef]
16. Ye, Y.-Y.; Qian, T.-T.; Jiang, H. Co loaded N-doped Biochar as a High Performance of Oxygen Reduction Reaction Electrocatalyst by Combined Pyrolysis of Biomass. *Ind. Eng. Chem. Res.* **2020**, *59*, 15614–15623. [CrossRef]
17. Garg, R.; Elmas, S.; Nann, T.; Andersson, M.R. Deposition methods of graphene as electrode material for organic solar cells. *Adv. Energy Mater.* **2016**, *7*, 1601393. [CrossRef]
18. Deng, J.; Li, M.; Wang, Y. Biomass-derived carbon: Synthesis and applications in energy storage and conversion. *Green Chem.* **2016**, *18*, 4824–4854. [CrossRef]
19. Deng, J.; Xiong, T.; Wang, H.; Zheng, A.; Wang, Y. Effects of cellulose, hemicellulose, and lignin on the structure and morphology of porous carbons. *ACS Sustain. Chem. Eng.* **2016**, *4*, 3750–3756. [CrossRef]
20. Chu, G.; Zhao, J.; Huang, Y.; Zhou, D.; Liu, Y.; Wu, M.; Peng, H.; Zhao, Q.; Pan, B.; Steinberg, C.E. Phosphoric acid pretreatment enhances the specific surface areas of biochars by generation of micropores. *Environ. Pollut.* **2018**, *240*, 1–9. [CrossRef]
21. Sharma, R.; Wooten, J.; Baliga, V.; Hajaligol, M. Characterization of chars from biomass-derived materials: Pectin chars. *Fuel* **2001**, *80*, 1825–1836. [CrossRef]
22. Matsagar, B.M.; Yang, R.-X.; Dutta, S.; Ok, Y.S.; Wu, K.C.-W. Recent progress in the development of biomass-derived nitrogen-doped porous carbon. *J. Mater. Chem. A* **2020**, *9*, 3703–3728. [CrossRef]
23. Sajjadi, B.; Chen, W.-Y.; Egiebor, N.O. A comprehensive review on physical activation of biochar for energy and environmental applications. *Rev. Chem. Eng.* **2018**, *35*, 735–776. [CrossRef]
24. Sajjadi, B.; Zubatiuk, T.; Leszczynska, D.; Leszczynski, J.; Chen, W.Y. Chemical activation of biochar for energy and environmental applications: A comprehensive review. *Rev. Chem. Eng.* **2018**, *35*, 777–815. [CrossRef]
25. Huang, W.-H.; Lee, D.-J.; Huang, C. Modification on biochars for applications: A research update. *Bioresour. Technol.* **2020**, *319*, 124100. [CrossRef] [PubMed]
26. Shen, F.; Xiong, X.; Fu, J.; Yang, J.; Qiu, M.; Qi, X.; Tsang, D.C. Recent advances in mechanochemical production of chemicals and carbon materials from sustainable biomass resources. *Renew. Sustain. Energy Rev.* **2020**, *130*, 109944. [CrossRef]
27. Gaudino, E.C.; Cravotto, G.; Manzoli, M.; Tabasso, S. Sono- and mechanochemical technologies in the catalytic conversion of biomass. *Chem. Soc. Rev.* **2020**, *50*, 1785–1812. [CrossRef]
28. Basu, P. *Biomass Gasification, Pyrolysis and Torrefaction: Practical Design and Theory*; Academic Press: Cambridge, MA, USA, 2018.
29. Xiu, S.; Shahbazi, A.; Li, R. Characterization, modification and application of biochar for energy storage and catalysis: A review. *Trends Renew. Energy* **2017**, *3*, 86–101. [CrossRef]
30. Kambo, H.S.; Dutta, A. A comparative review of biochar and hydrochar in terms of production, physico-chemical properties and applications. *Renew. Sustain. Energy Rev.* **2015**, *45*, 359–378. [CrossRef]
31. Alonso, D.M.; Wettstein, S.G.; Dumesic, J.A. Bimetallic catalysts for upgrading of biomass to fuels and chemicals. *Chem. Soc. Rev.* **2012**, *41*, 8075–8098. [CrossRef]
32. Leng, L.; Xiong, Q.; Yang, L.; Li, H.; Zhou, Y.; Zhang, W.; Jiang, S.; Li, H.; Huang, H. An overview on engineering the surface area and porosity of biochar. *Sci. Total Environ.* **2020**, *763*, 144204. [CrossRef]
33. Maggi, R.; Delmon, B. Comparison between 'slow'and 'flash'pyrolysis oils from biomass. *Fuel* **1994**, *73*, 671–677. [CrossRef]
34. Román, S.; Valente Nabais, J.M.; Ledesma, B.; González, J.F.; Laginhas, C.; Titirici, M.M. Production of low-cost adsorbents with tunable surface chemistry by conjunction of hydrothermal carbonization and activation processes. *Microporous Mesoporous Mater.* **2013**, *165*, 127–133. [CrossRef]
35. Panwar, N.L.; Pawar, A. Influence of activation conditions on the physicochemical properties of activated biochar: A review. *Biomass Convers. Biorefinery* **2020**, *12*, 925–947. [CrossRef]
36. Demirbaş, A. Mechanisms of liquefaction and pyrolysis reactions of biomass. *Energy Convers. Manag.* **2000**, *41*, 633–646. [CrossRef]
37. Goldstein, I.S. *Organic Chemicals from Biomass*; CRC Press: Boca Raton, FL, USA, 2018. [CrossRef]
38. Khan, S.R.; Zeeshan, M.; Masood, A. Enhancement of hydrocarbons production through co-pyrolysis of acid-treated biomass and waste tire in a fixed bed reactor. *Waste Manag.* **2020**, *106*, 21–31. [CrossRef] [PubMed]
39. Khan, S.R.; Zeeshan, M. Catalytic potential of low-cost natural zeolite and influence of various pretreatments of biomass on pyro-oil up-gradation during co-pyrolysis with scrap rubber tires. *Energy* **2021**, *238*, 121820. [CrossRef]
40. Ma, Z.; Yang, Y.; Wu, Y.; Xu, J.; Peng, H.; Liu, X.; Zhang, W.; Wang, S. In-depth comparison of the physicochemical characteristics of bio-char derived from biomass pseudo components: Hemicellulose, cellulose, and lignin. *J. Anal. Appl. Pyrolysis* **2019**, *140*, 195–204. [CrossRef]
41. Yang, H.; Yan, R.; Chen, H.; Lee, D.H.; Zheng, C. Characteristics of hemicellulose, cellulose and lignin pyrolysis. *Fuel* **2007**, *86*, 1781–1788. [CrossRef]
42. Sun, Y.; Yu, I.K.; Tsang, D.C.; Fan, J.; Clark, J.H.; Luo, G.; Zhang, S.; Khan, E.; Graham, N.J. Tailored design of graphitic biochar for high-efficiency and chemical-free microwave-assisted removal of refractory organic contaminants. *Chem. Eng. J.* **2020**, *398*, 125505. [CrossRef]

43. Tomczyk, A.; Sokołowska, Z.; Boguta, P. Biochar physicochemical properties: Pyrolysis temperature and feedstock kind effects. *Rev. Environ. Sci. Bio Technol.* **2020**, *19*, 191–215. [CrossRef]
44. Sun, K.; Kang, M.; Zhang, Z.; Jin, J.; Wang, Z.; Pan, Z.; Xu, D.; Wu, F.; Xing, B. Impact of deashing treatment on biochar structural properties and potential sorption mechanisms of phenanthrene. *Environ. Sci. Technol.* **2013**, *47*, 11473–11481. [CrossRef]
45. Antal, M.J.; Grønli, M. The art, science, and technology of charcoal production. *Ind. Eng. Chem. Res.* **2003**, *42*, 1619–1640. [CrossRef]
46. Kumar, J.V.; Pratt, B.C. Compositional analysis of some renewable biofuels. *Am. Lab.* **1996**, *28*, 15–20.
47. Irfan, M.; Chen, Q.; Yue, Y.; Pang, R.; Lin, Q.; Zhao, X.; Chen, H. Co-production of biochar, bio-oil and syngas from halophyte grass (*Achnatherum splendens* L.) under three different pyrolysis temperatures. *Bioresour. Technol.* **2016**, *211*, 457–463. [CrossRef] [PubMed]
48. Pallarés, J.; González-Cencerrado, A.; Arauzo, I. Production and characterization of activated carbon from barley straw by physical activation with carbon dioxide and steam. *Biomass Bioenergy* **2018**, *115*, 64–73. [CrossRef]
49. Lehmann, J.; Joseph, S. *Biochar for Environmental Management: Science, Technology and Implementation*; Routledge: Abingdon, UK, 2015.
50. Leng, L.; Huang, H. An overview of the effect of pyrolysis process parameters on biochar stability. *Bioresour. Technol.* **2018**, *270*, 627–642. [CrossRef]
51. Zhao, B.; O'Connor, D.; Zhang, J.; Peng, T.; Shen, Z.; Tsang, D.C.W.; Hou, D. Effect of pyrolysis temperature, heating rate, and residence time on rapeseed stem derived biochar. *J. Clean. Prod.* **2018**, *174*, 977–987. [CrossRef]
52. Chen, D.; Li, Y.; Cen, K.; Luo, M.; Li, H.; Lu, B. Pyrolysis polygeneration of poplar wood: Effect of heating rate and pyrolysis temperature. *Bioresour. Technol.* **2016**, *218*, 780–788. [CrossRef]
53. Bouchelta, C.; Medjram, M.S.; Zoubida, M.; Chekkat, F.A.; Ramdane, N.; Bellat, J.-P. Effects of pyrolysis conditions on the porous structure development of date pits activated carbon. *J. Anal. Appl. Pyrolysis* **2012**, *94*, 215–222. [CrossRef]
54. Liu, R.; Liu, G.; Yousaf, B.; Abbas, Q. Operating conditions-induced changes in product yield and characteristics during thermal-conversion of peanut shell to biochar in relation to economic analysis. *J. Clean. Prod.* **2018**, *193*, 479–490. [CrossRef]
55. Sakhiya, A.K.; Anand, A.; Kaushal, P. Production, activation, and applications of biochar in recent times. *Biochar* **2020**, *2*, 253–285. [CrossRef]
56. Sahoo, S.S.; Vijay, V.K.; Chandra, R.; Kumar, H. Production and characterization of biochar produced from slow pyrolysis of pigeon pea stalk and bamboo. *Clean. Eng. Technol.* **2021**, *3*, 100101. [CrossRef]
57. Sun, Y.; Gao, B.; Yao, Y.; Fang, J.; Zhang, M.; Zhou, Y.; Chen, H.; Yang, L. Effects of feedstock type, production method, and pyrolysis temperature on biochar and hydrochar properties. *Chem. Eng. J.* **2014**, *240*, 574–578. [CrossRef]
58. Malekshahian, M.; Hill, J.M. Effect of pyrolysis and CO_2 gasification pressure on the surface area and pore size distribution of petroleum coke. *Energy Fuels* **2011**, *25*, 5250–5256. [CrossRef]
59. Kan, T.; Strezov, V.; Evans, T.J. Lignocellulosic biomass pyrolysis: A review of product properties and effects of pyrolysis parameters. *Renew. Sustain. Energy Rev.* **2016**, *57*, 1126–1140. [CrossRef]
60. Salema, A.A.; Afzal, M.T. Numerical simulation of heating behaviour in biomass bed and pellets under multimode microwave system. *Int. J. Therm. Sci.* **2015**, *91*, 12–24. [CrossRef]
61. Namazi, A.B.; Allen, D.; Jia, C.Q. Probing microwave heating of lignocellulosic biomasses. *J. Anal. Appl. Pyrolysis* **2015**, *112*, 121–128. [CrossRef]
62. Zhang, T.; Walawender, W.P.; Fan, L.; Fan, M.; Daugaard, D.; Brown, R. Preparation of activated carbon from forest and agricultural residues through CO_2 activation. *Chem. Eng. J.* **2004**, *105*, 53–59. [CrossRef]
63. Lu, H.; Zhao, X.S. Biomass-derived carbon electrode materials for supercapacitors. *Sustain. Energy Fuels* **2017**, *1*, 1265–1281. [CrossRef]
64. Cheng, B.-H.; Zeng, R.J.; Jiang, H. Recent developments of post-modification of biochar for electrochemical energy storage. *Bioresour. Technol.* **2017**, *246*, 224–233. [CrossRef]
65. Liu, W.-J.; Jiang, H.; Yu, H.-Q. Development of biochar-based functional materials: Toward a sustainable platform carbon material. *Chem. Rev.* **2015**, *115*, 12251–12285. [CrossRef]
66. Gao, Z.; Zhang, Y.; Song, N.; Li, X. Biomass-derived renewable carbon materials for electrochemical energy storage. *Mater. Res. Lett.* **2016**, *5*, 69–88. [CrossRef]
67. Parveen, N.; Ansari, S.A.; Ansari, M.O.; Cho, M.H. Manganese dioxide nanorods intercalated reduced graphene oxide nanocomposite toward high performance electrochemical supercapacitive electrode materials. *J. Colloid Interface Sci.* **2017**, *506*, 613–619. [CrossRef] [PubMed]
68. Song, S.; Ma, F.; Wu, G.; Ma, D.; Geng, W.; Wan, J. Facile self-templating large scale preparation of biomass-derived 3D hierarchical porous carbon for advanced supercapacitors. *J. Mater. Chem. A* **2015**, *3*, 18154–18162. [CrossRef]
69. Sun, Q. Porous carbon material based on biomass prepared by MgO template method and ZnCl2 activation method as Electrode for high performance supercapacitor. *Int. J. Electrochem. Sci.* **2019**, *14*, 1–14. [CrossRef]
70. Qin, L. Porous carbon derived from pine nut shell prepared by steam activation for supercapacitor electrode material. *Int. J. Electrochem. Sci.* **2019**, 8907–8918. [CrossRef]

71. Zhang, Z.; He, J.; Tang, X.; Wang, Y.; Yang, B.; Wang, K.; Zhang, D. Supercapacitors based on a nitrogen doped hierarchical porous carbon fabricated by self-activation of biomass: Excellent rate capability and cycle stability. *Carbon Lett.* **2019**, *29*, 585–594. [CrossRef]
72. Sundriyal, S.; Shrivastav, V.; Pham, H.D.; Mishra, S.; Deep, A.; Dubal, D.P. Advances in bio-waste derived activated carbon for supercapacitors: Trends, challenges and prospective. *Resour. Conserv. Recycl.* **2021**, *169*, 105548. [CrossRef]
73. Osman, N.; Shamsuddin, N.; Uemura, Y. Activated carbon of oil palm empty fruit bunch (EFB); core and shaggy. *Procedia Eng.* **2016**, *148*, 758–764. [CrossRef]
74. Taer, E.; Iwantono; Manik, S.T.; Taslim, R.; Dahlan, D.; Deraman, M. Preparation of activated carbon monolith electrodes from sugarcane bagasse by physical and physical-chemical activation process for supercapacitor application. *Adv. Mater. Res.* **2014**, *896*, 179–182. [CrossRef]
75. Xiao, H.; Peng, H.; Deng, S.; Yang, X.; Zhang, Y.; Li, Y. Preparation of activated carbon from edible fungi residue by microwave assisted K_2CO_3 activation—application in reactive black 5 adsorption from aqueous solution. *Bioresour. Technol.* **2012**, *111*, 127–133. [CrossRef]
76. Januszewicz, K.; Cymann-Sachajdak, A.; Kazimierski, P.; Klein, M.; Łuczak, J.; Wilamowska-Zawłocka, M. Chestnut-derived activated carbon as a prospective material for energy storage. *Materials* **2020**, *13*, 4658. [CrossRef] [PubMed]
77. Li, Z.; Guo, D.; Liu, Y.; Wang, H.; Wang, L. Recent advances and challenges in biomass-derived porous carbon nanomaterials for supercapacitors. *Chem. Eng. J.* **2020**, *397*, 125418. [CrossRef]
78. Nabais, J.M.V.; Nunes, P.; Carrott, P.J.; Carrott MM, L.R.; García, A.M.; Díaz-Díez, M.A. Production of activated carbons from coffee endocarp by CO_2 and steam activation. *Fuel Processing Technol.* **2008**, *89*, 262–268. [CrossRef]
79. Aworn, A.; Thiravetyan, P.; Nakbanpote, W. Preparation and characteristics of agricultural waste activated carbon by physical activation having micro- and mesopores. *J. Anal. Appl. Pyrolysis* **2008**, *82*, 279–285. [CrossRef]
80. Bouchelta, C.; Medjram, M.S.; Bertrand, O.; Bellat, J.P. Preparation and characterization of activated carbon from date stones by physical activation with steam. *J. Anal. Appl. Pyrolysis* **2008**, *82*, 70–77. [CrossRef]
81. Cabal, B.; Budinova, T.; Ania, C.O.; Tsyntsarski, B.; Parra, J.B.; Petrova, B. Adsorption of naphthalene from aqueous solution on activated carbons obtained from bean pods. *J. Hazard. Mater.* **2009**, *161*, 1150–1156. [CrossRef]
82. Cagnon, B.; Py, X.; Guillot, A.; Stoeckli, F.; Chambat, G. Contributions of hemicellulose, cellulose and lignin to the mass and the porous properties of chars and steam activated carbons from various lignocellulosic precursors. *Bioresour. Technol.* **2009**, *100*, 292–298. [CrossRef]
83. Nabais, J.V.; Teixeira, J.G.; Almeida, I. Development of easy made low cost bindless monolithic electrodes from biomass with controlled properties to be used as electrochemical capacitors. *Bioresour. Technol.* **2011**, *102*, 2781–2787. [CrossRef]
84. Nabais, J.V.; Carrott, P.; Carrott, M.R.; Luz, V.; Ortiz, A.L. Influence of preparation conditions in the textural and chemical properties of activated carbons from a novel biomass precursor: The coffee endocarp. *Bioresour. Technol.* **2008**, *99*, 7224–7231. [CrossRef]
85. Haffner-Staton, E.; Balahmar, N.; Mokaya, R. High yield and high packing density porous carbon for unprecedented CO_2 capture from the first attempt at activation of air-carbonized biomass. *J. Mater. Chem. A* **2016**, *4*, 13324–13335. [CrossRef]
86. Niu, J.; Liu, M.; Xu, F.; Zhang, Z.; Dou, M.; Wang, F. Synchronously boosting gravimetric and volumetric performance: Biomass-derived ternary-doped microporous carbon nanosheet electrodes for supercapacitors. *Carbon* **2018**, *140*, 664–672. [CrossRef]
87. Shang, T.-X.; Ren, R.-Q.; Zhu, Y.-M.; Jin, X.-J. Oxygen- and nitrogen-co-doped activated carbon from waste particleboard for potential application in high-performance capacitance. *Electrochim. Acta* **2015**, *163*, 32–40. [CrossRef]
88. Zhang, W.; Xu, J.; Hou, D.; Yin, J.; Liu, D.; He, Y.; Lin, H. Hierarchical porous carbon prepared from biomass through a facile method for supercapacitor applications. *J. Colloid Interface Sci.* **2018**, *530*, 338–344. [CrossRef]
89. Abechi, S.E.; Gimba, C.E.; Uzairu, A.; Dallatu, Y.A. Preparation and characterization of activated carbon from palm kernel shell by chemical activation. *Res. J. Chem. Sci.* **2013**, *3*, 54–61.
90. González-García, P.; Centeno, T.A.; Urones-Garrote, E.; Ávila-Brande, D.; Otero-Díaz, L.C. Microstructure and surface properties of lignocellulosic-based activated carbons. *Appl. Surf. Sci.* **2013**, *265*, 731–737. [CrossRef]
91. Elmouwahidi, A.; Zapata-Benabithe, Z.; Carrasco-Marín, F.; Moreno-Castilla, C. Activated carbons from KOH-activation of argan (*Argania spinosa*) seed shells as supercapacitor electrodes. *Bioresour. Technol.* **2012**, *111*, 185–190. [CrossRef]
92. Zhang, X.; Fan, Q.; Qu, N.; Yang, H.; Wang, M.; Liu, A.; Yang, J. Ultrathin 2D nitrogen-doped carbon nanosheets for high performance supercapacitors: Insight into the effects of graphene oxides. *Nanoscale* **2019**, *11*, 8588–8596. [CrossRef]
93. Guo, Y.; Liu, W.; Wu, R.; Sun, L.; Zhang, Y.; Cui, Y.; Liu, S.; Wang, H.; Shan, B. Marine-biomass-derived porous carbon sheets with a tunable n-doping content for superior sodium-ion storage. *ACS Appl. Mater. Interfaces* **2018**, *10*, 38376–38386. [CrossRef]
94. Ramakrishnan, K.; Nithya, C.; Karvembu, R. High-performance sodium ion capacitor based on MoO_2@rGO nanocomposite and goat hair derived carbon electrodes. *ACS Appl. Energy Mater.* **2018**, *1*, 841–850. [CrossRef]
95. Qiao, Y.; Ma, M.; Liu, Y.; Li, S.; Lu, Z.; Yue, H.; Dong, H.; Cao, Z.; Yin, Y.; Yang, S. First-principles and experimental study of nitrogen/sulfur co-doped carbon nanosheets as anodes for rechargeable sodium ion batteries. *J. Mater. Chem. A* **2016**, *4*, 15565–15574. [CrossRef]
96. Yang, K.; Peng, J.; Srinivasakannan, C.; Zhang, L.; Xia, H.; Duan, X. Preparation of high surface area activated carbon from coconut shells using microwave heating. *Bioresour. Technol.* **2010**, *101*, 6163–6169. [CrossRef] [PubMed]

97. Tay, T.; Ucar, S.; Karagöz, S. Preparation and characterization of activated carbon from waste biomass. *J. Hazard. Mater.* **2009**, *165*, 481–485. [CrossRef] [PubMed]
98. Jin, H.; Wang, X.; Gu, Z.; Polin, J. Carbon materials from high ash biochar for supercapacitor and improvement of capacitance with HNO_3 surface oxidation. *J. Power Sources* **2013**, *236*, 285–292. [CrossRef]
99. Liu, Y.; Huang, B.; Lin, X.; Xie, Z. Correction: Biomass-derived hierarchical porous carbons: Boosting the energy density of supercapacitors via an ionothermal approach. *J. Mater. Chem. A* **2017**, *5*, 25090. [CrossRef]
100. Chen, C.; Yu, D.; Zhao, G.; Du, B.; Tang, W.; Sun, L.; Sun, Y.; Besenbacher, F.; Yu, M. Three-dimensional scaffolding framework of porous carbon nanosheets derived from plant wastes for high-performance supercapacitors. *Nano Energy* **2016**, *27*, 377–389. [CrossRef]
101. Yu, H.; Zhang, W.; Li, T.; Zhi, L.; Dang, L.; Liu, Z.; Lei, Z. Capacitive performance of porous carbon nanosheets derived from biomass cornstalk. *RSC Adv.* **2017**, *7*, 1067–1074. [CrossRef]
102. Wang, P.; Zhang, G.; Li, M.-Y.; Yin, Y.-X.; Li, J.-Y.; Li, G.; Wang, W.-P.; Peng, W.; Cao, F.-F.; Guo, Y.-G. Porous carbon for high-energy density symmetrical supercapacitor and lithium-ion hybrid electrochemical capacitors. *Chem. Eng. J.* **2019**, *375*, 122020. [CrossRef]
103. Raj, C.J.; Rajesh, M.; Manikandan, R.; Yu, K.H.; Anusha, J.; Ahn, J.H.; Kim, D.-W.; Park, S.Y.; Kim, B.C. High electrochemical capacitor performance of oxygen and nitrogen enriched activated carbon derived from the pyrolysis and activation of squid gladius chitin. *J. Power Sources* **2018**, *386*, 66–76. [CrossRef]
104. Yu, D.; Ma, Y.; Chen, M.; Dong, X. KOH activation of wax gourd-derived carbon materials with high porosity and heteroatom content for aqueous or all-solid-state supercapacitors. *J. Colloid Interface Sci.* **2018**, *537*, 569–578. [CrossRef]
105. Chen, J.; Zhou, X.; Mei, C.; Xu, J.; Zhou, S.; Wong, C.-P. Evaluating biomass-derived hierarchically porous carbon as the positive electrode material for hybrid Na-ion capacitors. *J. Power Sources* **2017**, *342*, 48–55. [CrossRef]
106. Yang, G.; Park, S.-J. MnO_2 and biomass-derived 3D porous carbon composites electrodes for high performance supercapacitor applications. *J. Alloys Compd.* **2018**, *741*, 360–367. [CrossRef]
107. Takeuchi, K.; Fujishige, M.; Ishida, N.; Kunieda, Y.; Kato, Y.; Tanaka, Y.; Ochi, T.; Shirotori, H.; Uzuhashi, Y.; Ito, S.; et al. High porous bio-nanocarbons prepared by carbonization and NaOH activation of polysaccharides for electrode material of EDLC. *J. Phys. Chem. Solids* **2018**, *118*, 137–143. [CrossRef]
108. Zhou, L.; Cao, H.; Zhu, S.; Hou, L.; Yuan, C. Hierarchical micro-/mesoporous N-and O-enriched carbon derived from disposable cashmere: A competitive cost-effective material for high-performance electrochemical capacitors. *Green Chem.* **2015**, *17*, 2373–2382. [CrossRef]
109. Cruz, G.; Pirilä, M.; Huuhtanen, M.; Carrión, L.; Alvarenga, E.; Keiski, R.L. Production of Activated Carbon from Cocoa (*Theobroma cacao*) Pod Husk. *J. Civ. Environ. Eng.* **2012**, *2*, 1–6. [CrossRef]
110. Selvaraj, A.R.; Chinnadurai, D.; Cho, I.; Bak, J.S.; Prabakar, K. Bio-waste wood-derived porous activated carbon with tuned microporosity for high performance supercapacitors. *J. Energy Storage* **2022**, *52*, 104928. [CrossRef]
111. Kumagai, S.; Tashima, D. Electrochemical performance of activated carbons prepared from rice husk in different types of non-aqueous electrolytes. *Biomass Bioenergy* **2015**, *83*, 216–223. [CrossRef]
112. Chen, L.; Ji, T.; Mu, L.; Zhu, J. Cotton fabric derived hierarchically porous carbon and nitrogen doping for sustainable capacitor electrode. *Carbon* **2017**, *111*, 839–848. [CrossRef]
113. Libich, J.; Máca, J.; Vondrák, J.; Čech, O.; Sedlaříková, M. Supercapacitors: Properties and applications. *J. Energy Storage* **2018**, *17*, 224–227. [CrossRef]
114. Du, J.; Liu, L.; Hu, Z.; Yu, Y.; Zhang, Y.; Hou, S.; Chen, A. Raw-cotton-derived n-doped carbon fiber aerogel as an efficient electrode for electrochemical capacitors. *ACS Sustain. Chem. Eng.* **2018**, *6*, 4008–4015. [CrossRef]
115. Wei, X.; Wan, S.; Gao, S. Self-assembly-template engineering nitrogen-doped carbon aerogels for high-rate supercapacitors. *Nano Energy* **2016**, *28*, 206–215. [CrossRef]
116. Ding, J.; Wang, H.; Li, Z.; Cui, K.; Karpuzov, D.; Tan, X.; Kohandehghan, A.; Mitlin, D. Peanut shell hybrid sodium ion capacitor with extreme energy–power rivals lithium ion capacitors. *Energy Environ. Sci.* **2014**, *8*, 941–955. [CrossRef]
117. Im, U.-S.; Kim, J.; Lee, S.H.; Lee, S.M.; Lee, B.-R.; Peck, D.-H.; Jung, D.-H. Preparation of activated carbon from needle coke via two-stage steam activation process. *Mater. Lett.* **2018**, *237*, 22–25. [CrossRef]
118. Ismanto, A.E.; Wang, S.; Soetaredjo, F.E.; Ismadji, S. Preparation of capacitor's electrode from cassava peel waste. *Bioresour. Technol.* **2010**, *101*, 3534–3540. [CrossRef] [PubMed]
119. Williams, P.; Reed, A. Development of activated carbon pore structure via physical and chemical activation of biomass fibre waste. *Biomass Bioenergy* **2006**, *30*, 144–152. [CrossRef]
120. Abioye, A.M.; Ani, F.N. Recent development in the production of activated carbon electrodes from agricultural waste biomass for supercapacitors: A review. *Renew. Sustain. Energy Rev.* **2015**, *52*, 1282–1293. [CrossRef]
121. Cuong, D.V.; Liu, N.-L.; Nguyen, V.A.; Hou, C.-H. Meso/micropore-controlled hierarchical porous carbon derived from activated biochar as a high-performance adsorbent for copper removal. *Sci. Total Environ.* **2019**, *692*, 844–853. [CrossRef]
122. Jiang, C.; Yakaboylu, G.A.; Yumak, T.; Zondlo, J.W.; Sabolsky, E.M.; Wang, J. Activated carbons prepared by indirect and direct CO_2 activation of lignocellulosic biomass for supercapacitor electrodes. *Renew. Energy* **2020**, *155*, 38–52. [CrossRef]
123. Olorundare, O.F.; Msagati, T.; Krause, R.W.M.; Okonkwo, J.O.; Mamba, B.B. Activated Carbon from lignocellulosic waste residues: Effect of activating agent on porosity characteristics and use as adsorbents for organic species. *Water Air Soil Pollut.* **2014**, *225*, 1876. [CrossRef]

124. Girgis, B.S.; Soliman, A.M.; Fathy, N.A. Development of micro-mesoporous carbons from several seed hulls under varying conditions of activation. *Microporous Mesoporous Mater.* **2011**, *142*, 518–525. [CrossRef]
125. Qian, L.; Guo, F.; Jia, X.; Zhan, Y.; Zhou, H.; Jiang, X.; Tao, C. Recent development in the synthesis of agricultural and forestry biomass-derived porous carbons for supercapacitor applications: A review. *Ionics* **2020**, *26*, 3705–3723. [CrossRef]
126. Fu, K.; Yue, Q.; Gao, B.; Sun, Y.; Zhu, L. Preparation, characterization and application of lignin-based activated carbon from black liquor lignin by steam activation. *Chem. Eng. J.* **2013**, *228*, 1074–1082. [CrossRef]
127. Suhas; Carrott, P.; Carrott, M.R.; Singh, R.; Singh, L.; Chaudhary, M. An innovative approach to develop microporous activated carbons in oxidising atmosphere. *J. Clean. Prod.* **2017**, *156*, 549–555. [CrossRef]
128. Vinayagam, M.; Babu, R.S.; Sivasamy, A.; de Barros, A.L.F. Biomass-derived porous activated carbon from Syzygium cumini fruit shells and Chrysopogon zizanioides roots for high-energy density symmetric supercapacitors. *Biomass Bioenergy* **2020**, *143*, 105838. [CrossRef]
129. Lim, W.; Srinivasakannan, C.; Balasubramanian, N. Activation of palm shells by phosphoric acid impregnation for high yielding activated carbon. *J. Anal. Appl. Pyrolysis* **2010**, *88*, 181–186. [CrossRef]
130. Gunasekaran, S.S.; Badhulika, S. High-performance solid-state supercapacitor based on sustainable synthesis of meso-macro porous carbon derived from hemp fibres via CO_2 activation. *J. Energy Storage* **2021**, *41*, 102997. [CrossRef]
131. Ahmida, K.; Darmoon, M.; Al-Tohami, F.; Erhayem, M.; Zidan, M. Effect of Physical and Chemical Preparation on Characteristics of Activated Carbon from Agriculture Solid Waste and Their Potential Application. In Proceedings of the International Conference on Chemical, Civil and Environmental Engineering, Istanbul, Turkey, 5–6 June 2015.
132. Sarwar, A.; Ali, M.; Khoja, A.H.; Nawar, A.; Waqas, A.; Liaquat, R.; Naqvi, S.R.; Asjid, M. Synthesis and characterization of biomass-derived surface-modified activated carbon for enhanced CO_2 adsorption. *J. CO_2 Util.* **2021**, *46*, 101476. [CrossRef]
133. Hesas, R.H.; Arami-Niya, A.; Daud, W.M.A.W.; Sahu, J.N. Preparation of granular activated carbon from oil palm shell by microwave-induced chemical activation: Optimisation using surface response methodology. *Chem. Eng. Res. Des.* **2013**, *91*, 2447–2456. [CrossRef]
134. Sevilla, M.; Fuertes, A.B.; Mokaya, R. High density hydrogen storage in superactivated carbons from hydrothermally carbonized renewable organic materials. *Energy Environ. Sci.* **2011**, *4*, 1400–1410. [CrossRef]
135. Dehkhoda, A.M.; Gyenge, E.; Ellis, N. A novel method to tailor the porous structure of KOH-activated biochar and its application in capacitive deionization and energy storage. *Biomass Bioenergy* **2016**, *87*, 107–121. [CrossRef]
136. Zhang, Y.-L.; Li, S.-Y.; Tang, Z.-S.; Song, Z.-X.; Sun, J. Xanthoceras sorbifolia seed coats derived porous carbon with unique architecture for high rate performance supercapacitors. *Diam. Relat. Mater.* **2018**, *91*, 119–126. [CrossRef]
137. Zhang, G.; Chen, Y.; Chen, Y.; Guo, H. Activated biomass carbon made from bamboo as electrode material for supercapacitors. *Mater. Res. Bull.* **2018**, *102*, 391–398. [CrossRef]
138. Li, Y.; Yu, N.; Yan, P.; Li, Y.; Zhou, X.; Chen, S.; Wang, G.; Wei, T.; Fan, Z. Fabrication of manganese dioxide nanoplates anchoring on biomass-derived cross-linked carbon nanosheets for high-performance asymmetric supercapacitors. *J. Power Sources* **2015**, *300*, 309–317. [CrossRef]
139. Sudhan, N.; Subramani, K.; Karnan, M.; Ilayaraja, N.; Sathish, M. Biomass-derived activated porous carbon from rice straw for a high-energy symmetric supercapacitor in aqueous and non-aqueous electrolytes. *Energy Fuels* **2016**, *31*, 977–985. [CrossRef]
140. Deng, J.; Xiong, T.; Xu, F.; Li, M.; Han, C.; Gong, Y.; Wang, H.; Wang, Y. Inspired by bread leavening: One-pot synthesis of hierarchically porous carbon for supercapacitors. *Green Chem.* **2015**, *17*, 4053–4060. [CrossRef]
141. Sevilla, M.; Mokaya, R. Energy storage applications of activated carbons: Supercapacitors and hydrogen storage. *Energy Environ. Sci.* **2014**, *7*, 1250–1280. [CrossRef]
142. Zhao, S.; Wang, C.-Y.; Chen, M.-M.; Wang, J.; Shi, Z.-Q. Potato starch-based activated carbon spheres as electrode material for electrochemical capacitor. *J. Phys. Chem. Solids* **2009**, *70*, 1256–1260. [CrossRef]
143. Kim, Y.-J.; Lee, B.-J.; Suezaki, H.; Chino, T.; Abe, Y.; Yanagiura, T.; Park, K.C.; Endo, M. Preparation and characterization of bamboo-based activated carbons as electrode materials for electric double layer capacitors. *Carbon* **2006**, *44*, 1592–1595. [CrossRef]
144. Wang, D.; Geng, Z.; Li, B.; Zhang, C. High performance electrode materials for electric double-layer capacitors based on biomass-derived activated carbons. *Electrochim. Acta* **2015**, *173*, 377–384. [CrossRef]
145. Arami-Niya, A.; Daud, W.M.A.W.; Mjalli, F.S.; Abnisa, F.; Shafeeyan, M.S. Production of microporous palm shell based activated carbon for methane adsorption: Modeling and optimization using response surface methodology. *Chem. Eng. Res. Des.* **2012**, *90*, 776–784. [CrossRef]
146. Ooi, C.-H.; Cheah, W.-K.; Sim, Y.-L.; Pung, S.-Y.; Yeoh, F.-Y. Conversion and characterization of activated carbon fiber derived from palm empty fruit bunch waste and its kinetic study on urea adsorption. *J. Environ. Manag.* **2017**, *197*, 199–205. [CrossRef]
147. Chowdhury, Z.Z.; Hamid, S.B.A.; Das, R.; Hasan, R.; Zain, S.M.; Khalid, K.; Uddin, N. Preparation of carbonaceous adsorbents from lignocellulosic biomass and their use in removal of contaminants from aqueous solution. *BioResources* **2013**, *8*, 6523–6555. [CrossRef]
148. Hu, Z.; Guo, H.; Srinivasan, M.; Yaming, N. A simple method for developing mesoporosity in activated carbon. *Sep. Purif. Technol.* **2003**, *31*, 47–52. [CrossRef]
149. Yuliusman; Nasruddin; Afdhol, M.K.; Haris, F.; Amiliana, R.A.; Hanafi, A.; Ramadhan, I.T. Production of activated carbon from coffee grounds using chemical and physical activation method. *Adv. Sci. Lett.* **2017**, *23*, 5751–5755. [CrossRef]

150. Li, X.; Zhang, J.; Liu, B.; Su, Z. A critical review on the application and recent developments of post-modified biochar in supercapacitors. *J. Clean. Prod.* **2021**, *310*, 127428. [CrossRef]
151. Peng, L.; Liang, Y.; Huang, J.; Xing, L.; Hu, H.; Xiao, Y.; Dong, H.; Liu, Y.; Zheng, M. Mixed-biomass wastes derived hierarchically porous carbons for high-performance electrochemical energy storage. *ACS Sustain. Chem. Eng.* **2019**, *7*, 10393–10402. [CrossRef]
152. Rani, M.U.; Nanaji, K.; Rao, T.N.; Deshpande, A.S. Corn husk derived activated carbon with enhanced electrochemical performance for high-voltage supercapacitors. *J. Power Sources* **2020**, *471*, 228387. [CrossRef]
153. Liu, D.; Zhang, W.; Huang, W. Effect of removing silica in rice husk for the preparation of activated carbon for supercapacitor applications. *Chin. Chem. Lett.* **2019**, *30*, 1315–1319. [CrossRef]
154. Zhang, J.; Gong, L.; Sun, K.; Jiang, J.; Zhang, X. Preparation of activated carbon from waste Camellia oleifera shell for supercapacitor application. *J. Solid State Electrochem.* **2012**, *16*, 2179–2186. [CrossRef]
155. Khan, A.; Senthil, R.A.; Pan, J.; Sun, Y.; Liu, X.; Pan, Y. Hierarchically porous biomass carbon derived from natural withered rose flowers as high-performance material for advanced supercapacitors. *Batter. Supercaps* **2020**, *3*, 731–737. [CrossRef]
156. Li, X.; Xing, W.; Zhuo, S.; Zhou, J.; Li, F.; Qiao, S.Z.; Lu, G.Q. Preparation of capacitor's electrode from sunflower seed shell. *Bioresour. Technol.* **2011**, *102*, 1118–1123. [CrossRef]
157. Gao, Y.; Li, L.; Jin, Y.; Wang, Y.; Yuan, C.; Wei, Y.; Chen, G.; Ge, J.; Lu, H. Porous carbon made from rice husk as electrode material for electrochemical double layer capacitor. *Appl. Energy* **2015**, *153*, 41–47. [CrossRef]
158. Teo, E.Y.L.; Muniandy, L.; Ng, E.-P.; Adam, F.; Mohamed, A.R.; Jose, R.; Chong, K.F. High surface area activated carbon from rice husk as a high performance supercapacitor electrode. *Electrochim. Acta* **2016**, *192*, 110–119. [CrossRef]
159. Song, J.; Shen, W.; Wang, J.; Fan, W. Hierarchical Porous Carbons Derived from Renewable Poplar Anthers for High-Performance Supercapacitors. *ChemElectroChem* **2018**, *5*, 1451–1458. [CrossRef]
160. Xu, B.; Chen, Y.; Wei, G.; Cao, G.; Zhang, H.; Yang, Y. Activated carbon with high capacitance prepared by NaOH activation for supercapacitors. *Mater. Chem. Phys.* **2010**, *124*, 504–509. [CrossRef]
161. Luo, J.; Zhang, H.; Zhanga, Z.; Yua, J.; Yangab, Z. In-built template synthesis of hierarchical porous carbon microcubes from biomass toward electrochemical energy storage. *Carbon* **2019**, *155*, 1–8. [CrossRef]
162. Okonkwo, C.A.; Lv, T.; Hong, W.; Li, G.; Huang, J.; Deng, J.; Jia, L.; Wu, M.; Liu, H.; Guo, M. The synthesis of micromesoporous carbon derived from nitrogen-rich spirulina extract impregnated castor shell based on biomass self-doping for highly efficient supercapacitor electrodes. *J. Alloys Compd.* **2020**, *825*, 154009. [CrossRef]
163. Li, Y.; Zhang, D.; Zhang, Y.; He, J.; Wang, Y.; Wang, K.; Xu, Y.; Li, H.; Wang, Y. Biomass-derived microporous carbon with large micropore size for high-performance supercapacitors. *J. Power Sources* **2020**, *448*, 227369. [CrossRef]
164. Chen, H.; Wang, G.; Chen, L.; Dai, B.; Yu, F. Three-dimensional honeycomb-like porous carbon with both interconnected hierarchical porosity and nitrogen self-doping from cotton seed husk for supercapacitor electrode. *Nanomaterials* **2018**, *8*, 412. [CrossRef] [PubMed]
165. Tian, X.; Ma, H.; Li, Z.; Yan, S.; Ma, L.; Yu, F.; Wang, G.; Guo, X.; Ma, Y.; Wong, C. Flute type micropores activated carbon from cotton stalk for high performance supercapacitors. *J. Power Sources* **2017**, *359*, 88–96. [CrossRef]
166. Peng, C.; Yan, X.B.; Wang, R.T.; Lang, J.W.; Ou, Y.J.; Xue, Q.J. Promising activated carbons derived from waste tea-leaves and their application in high performance supercapacitors electrodes. *Electrochim. Acta* **2013**, *87*, 401–408. [CrossRef]
167. Balathanigaimani, M.S.; Shim, W.G.; Lee, M.J.; Kim, C.; Lee, J.W.; Moon, H. Highly porous electrodes from novel corn grains-based activated carbons for electrical double layer capacitors. *Electrochem. Commun.* **2008**, *10*, 868–871. [CrossRef]
168. Sun, Y.; Xue, J.; Dong, S.; Zhang, Y.; An, Y.; Ding, B.; Zhang, T.; Dou, H.; Zhang, X. Biomass-derived porous carbon electrodes for high-performance supercapacitors. *J. Mater. Sci.* **2020**, *55*, 5166–5176. [CrossRef]
169. Ahmad, M.; Usman, A.R.; Al-Faraj, A.S.; Abduljabbar, A.; Ok, Y.S.; Al-Wabel, M.I. Date palm waste-derived biochar composites with silica and zeolite: Synthesis, characterization and implication for carbon stability and recalcitrant potential. *Environ. Geochem. Health* **2019**, *41*, 1687–1704. [CrossRef]
170. Lim, Y.S.; Lai, C.W.; Abd Hamid, S.B. Porous 3D carbon decorated Fe_3O_4 nanocomposite electrode for highly symmetrical supercapacitor performance. *RSC Adv.* **2017**, *7*, 23030–23040. [CrossRef]
171. Norouzi, O.; Pourhosseini, S.E.M.; Naderi, H.R.; Di Maria, F.; Dutta, A. Integrated hybrid architecture of metal and biochar for high performance asymmetric supercapacitors. *Sci. Rep.* **2021**, *11*, 1–13. [CrossRef]
172. Sharma, K.; Arora, A.; Tripathi, S.K. Review of supercapacitors: Materials and devices. *J. Energy Storage* **2019**, *21*, 801–825. [CrossRef]
173. Pourhosseini, S.; Norouzi, O.; Naderi, H.R. Study of micro/macro ordered porous carbon with olive-shaped structure derived from Cladophora glomerata macroalgae as efficient working electrodes of supercapacitors. *Biomass Bioenergy* **2017**, *107*, 287–298. [CrossRef]
174. Pourhosseini, S.E.M.; Norouzisafsari, O.; Salimi, P.; Naderi, H.R. Synthesis of a novel interconnected 3D pore network algal biochar constituting iron nanoparticles derived from a harmful marine biomass as high-performance asymmetric supercapacitor electrodes. *ACS Sustain. Chem. Eng.* **2018**, *6*, 4746–4758. [CrossRef]
175. Zhi, M.; Xiang, C.; Li, J.; Li, M.; Wu, N. Nanostructured carbon–metal oxide composite electrodes for supercapacitors: A review. *Nanoscale* **2013**, *5*, 72–88. [CrossRef]
176. Thomas, D.; Fernandez, N.B.; Mullassery, M.D.; Surya, R. Iron oxide loaded biochar/polyaniline nanocomposite: Synthesis, characterization and electrochemical analysis. *Inorg. Chem. Commun.* **2020**, *119*, 108097. [CrossRef]

177. Borenstein, A.; Hanna, O.; Attias, R.; Luski, S.; Brousse, T.; Aurbach, D. Carbon-based composite materials for supercapacitor electrodes: A review. *J. Mater. Chem. A* **2017**, *5*, 12653–12672. [CrossRef]
178. Li, X.; Zhou, J.; Li, X.; Xin, M.; Cai, T.; Xing, W.; Chai, Y.; Xue, Q.; Yan, Z. Bifuntional petaloid nickel manganese layered double hydroxides decorated on a freestanding carbon foam for flexible asymmetric supercapacitor and oxygen evolution. *Electrochim. Acta* **2017**, *252*, 275–285. [CrossRef]
179. Anjali, J.; Jose, V.K.; Lee, J.-M. Carbon-based hydrogels: Synthesis and their recent energy applications. *J. Mater. Chem. A* **2019**, *7*, 15491–15518. [CrossRef]
180. Tan, S.; Kraus, T.J.; Li-Oakey, K.D. Understanding the supercapacitor properties of electrospun carbon nanofibers from Powder River Basin coal. *Fuel* **2019**, *245*, 148–159. [CrossRef]
181. Deng, Y.; Ji, Y.; Wu, H.; Chen, F. Enhanced electrochemical performance and high voltage window for supercapacitor based on multi-heteroatom modified porous carbon materials. *Chem. Commun.* **2018**, *55*, 1486–1489. [CrossRef]
182. Karamanova, B.; Stoyanova, R.; Shipochka, M.; Girginov, C. On the cycling stability of biomass-derived carbons as electrodes in supercapacitors. *J. Alloys Compd.* **2019**, *803*, 882–890. [CrossRef]
183. Yu, X.; Zhao, J.; Lv, R.; Liang, Q.; Zhan, C.; Bai, Y.; Huang, Z.-H.; Shen, W.; Kang, F. Facile synthesis of nitrogen-doped carbon nanosheets with hierarchical porosity for high performance supercapacitors and lithium–sulfur batteries. *J. Mater. Chem. A* **2015**, *3*, 18400–18405. [CrossRef]
184. Li, J.; Liu, K.; Gao, X.; Yao, B.; Huo, K.; Cheng, Y.; Cheng, X.; Chen, D.; Wang, B.; Sun, W.; et al. Oxygen-and nitrogen-enriched 3D porous carbon for supercapacitors of high volumetric capacity. *ACS Appl. Mater. Interfaces* **2015**, *7*, 24622–24628. [CrossRef]
185. Lian, J.; Xiong, L.; Cheng, R.; Pang, D.; Tian, X.; Lei, J.; He, R.; Yu, X.; Duan, T.; Zhu, W. Ultra-high nitrogen content biomass carbon supercapacitors and nitrogen forms analysis. *J. Alloys Compd.* **2019**, *809*, 151664. [CrossRef]
186. Lyu, L.; Seong, K.-D.; Ko, D.; Choi, J.; Lee, C.; Hwang, T.; Cho, Y.; Jin, X.; Zhang, W.; Pang, H.; et al. Recent development of biomass-derived carbons and composites as electrode materials for supercapacitors. *Mater. Chem. Front.* **2019**, *3*, 2543–2570. [CrossRef]
187. Lai, F.; Miao, Y.-E.; Zuo, L.; Lu, H.; Huang, Y.; Liu, T. Biomass-Derived Nitrogen-Doped Carbon Nanofiber Network: A Facile Template for Decoration of Ultrathin Nickel-Cobalt Layered Double Hydroxide Nanosheets as High-Performance Asymmetric Supercapacitor Electrode. *Small* **2016**, *12*, 3235–3244. [CrossRef]
188. Deng, S.; Ai, C.; Luo, M.; Liu, B.; Zhang, Y.; Li, Y.; Lin, S.; Pan, G.; Xiong, Q.; Liu, Q.; et al. Coupled biphase (1T-2H)-$MoSe_2$ on mold spore carbon for advanced hydrogen evolution reaction. *Small* **2019**, *15*, 1901796. [CrossRef] [PubMed]
189. Yu, F.; Li, S.; Chen, W.; Wu, T.; Peng, C. Biomass-derived materials for electrochemical energy storage and conversion: Overview and perspectives. *Energy Environ. Mater.* **2019**, *2*, 55–67. [CrossRef]
190. Vijayakumar, M.; Sankar, A.B.; Rohita, D.S.; Rao, T.N.; Karthik, M. Conversion of biomass waste into high performance supercapacitor electrodes for real-time supercapacitor applications. *ACS Sustain. Chem. Eng.* **2019**, *7*, 17175–17185. [CrossRef]
191. Chen, D.; Yang, L.; Li, J.; Wu, Q. Effect of Self-Doped Heteroatoms in Biomass-Derived Activated Carbon for Supercapacitor Applications. *ChemistrySelect* **2019**, *4*, 1586–1595. [CrossRef]
192. Sankar, S.; Ahmed, A.T.A.; Inamdar, A.I.; Im, H.; Bin Im, Y.; Lee, Y.; Kim, D.Y.; Lee, S. Biomass-derived ultrathin mesoporous graphitic carbon nanoflakes as stable electrode material for high-performance supercapacitors. *Mater. Des.* **2019**, *169*, 107688. [CrossRef]
193. Huang, S.; Ding, Y.; Li, Y.; Han, X.; Xing, B.; Wang, S. Nitrogen and Sulfur Co-doped Hierarchical Porous Biochar Derived from the Pyrolysis of Mantis Shrimp Shell for Supercapacitor Electrodes. *Energy Fuels* **2021**, *35*, 1557–1566. [CrossRef]
194. Norouzi, O.; Di Maria, F.; Dutta, A. Biochar-based composites as electrode active materials in hybrid supercapacitors with particular focus on surface topography and morphology. *J. Energy Storage* **2020**, *29*, 101291. [CrossRef]
195. Zhou, B.; Sui, Y.; Qi, J.; He, Y.; Meng, Q.; Wei, F.; Ren, Y.; Zhang, X. Synthesis of Ultrathin MnO_2 Nanosheets/Bagasse Derived Porous Carbon Composite for Supercapacitor with High Performance. *J. Electron. Mater.* **2019**, *48*, 3026–3035. [CrossRef]
196. Golmohammadi, F.; Amiri, M. Facile synthesis of nanofiber composite based on biomass-derived material conjugated with nanoparticles of Ni–Co oxides for high-performance supercapacitors. *J. Mater. Sci. Mater. Electron.* **2020**, *31*, 2269–2279. [CrossRef]
197. Jiang, X.; Shi, G.; Wang, G.; Mishra, P.; Du, J.; Zhang, Y. Fe_2O_3/hemp straw-based porous carbon composite for supercapacitor electrode materials. *Ionics* **2020**, *26*, 4039–4051. [CrossRef]
198. Shang, Z.; An, X.; Zhang, H.; Shen, M.; Baker, F.; Liu, Y.; Liu, L.; Yang, J.; Cao, H.; Xu, Q.; et al. Houttuynia-derived nitrogen-doped hierarchically porous carbon for high-performance supercapacitor. *Carbon* **2020**, *161*, 62–70. [CrossRef]
199. Raj, F.R.M.S.; Boopathi, G.; Jaya, N.V.; Kalpana, D.; Pandurangan, A. N, S codoped activated mesoporous carbon derived from the Datura metel seed pod as active electrodes for supercapacitors. *Diam. Relat. Mater.* **2019**, *102*, 107687. [CrossRef]
200. Nirosha, B.; Selvakumar, R.; Jeyanthi, J.; Vairam, S. *Elaeocarpus tectorius* derived phosphorus-doped carbon as an electrode material for an asymmetric supercapacitor. *New J. Chem.* **2019**, *44*, 181–193. [CrossRef]
201. Meng, X.; Jia, S.; Mo, L.; Wei, J.; Wang, F.; Shao, Z. O/N-co-doped hierarchically porous carbon from carboxymethyl cellulose ammonium for high-performance supercapacitors. *J. Mater. Sci.* **2020**, *55*, 7417–7431. [CrossRef]
202. Wang, Q.; Zhang, Y.; Xiao, J.; Jiang, H.; Hu, T.; Meng, C. Copper oxide/cuprous oxide/hierarchical porous biomass-derived carbon hybrid composites for high-performance supercapacitor electrode. *J. Alloys Compd.* **2018**, *782*, 1103–1113. [CrossRef]
203. Wan, L.; Hu, J.; Liu, J.; Xie, M.; Zhang, Y.; Chen, J.; Du, C.; Tian, Z. Heteroatom-doped porous carbons derived from lotus pollen for supercapacitors: Comparison of three activators. *J. Alloys Compd.* **2020**, *859*, 158390. [CrossRef]

204. Xu, H.; Yan, X.-H.; Meng, Z.; Xue, T.; Li, D.; Fang, G.; Shen, H. Nitrogen-doped mesoporous carbon/poly-o-phenylenediamine composites for high-performance hybrid supercapacitor electrodes. *Mater. Res. Express* **2019**, *6*, 095601. [CrossRef]
205. Wan, L.; Wei, W.; Xie, M.; Zhang, Y.; Li, X.; Xiao, R.; Chen, J.; Du, C. Nitrogen, sulfur co-doped hierarchically porous carbon from rape pollen as high-performance supercapacitor electrode. *Electrochim. Acta* **2019**, *311*, 72–82. [CrossRef]
206. Wang, Y.; Shao, C.; Qiu, S.; Zhu, Y.; Qin, M.; Meng, Y.; Wang, Y.; Chu, H.; Zou, Y.; Xiang, C. Nitrogen-doped porous carbon derived from ginkgo leaves with remarkable supercapacitance performance. *Diam. Relat. Mater.* **2019**, *98*, 107475. [CrossRef]
207. Lei, W.; Yang, B.; Sun, Y.; Xiao, L.; Tang, D.; Chen, K.; Sun, J.; Ke, J.; Zhuang, Y. Self-sacrificial template synthesis of heteroatom doped porous biochar for enhanced electrochemical energy storage. *J. Power Sources* **2021**, *488*, 229455. [CrossRef]
208. Yang, X.; Jiang, Z.; Fei, B.; Ma, J.; Liu, X. Graphene functionalized bio-carbon xerogel for achieving high-rate and high-stability supercapacitors. *Electrochim. Acta* **2018**, *282*, 813–821. [CrossRef]
209. Yao, L.; Yang, J.; Zhang, P.; Deng, L. In situ surface decoration of $Fe_3C/Fe_3O_4/C$ nanosheets: Towards bi-functional activated carbons with supercapacitance and efficient dye adsorption. *Bioresour. Technol.* **2018**, *256*, 208–215. [CrossRef] [PubMed]
210. Shang, M.; Zhang, J.; Liu, X.; Liu, Y.; Guo, S.; Yu, S.; Filatov, S.; Yi, X. N, S self-doped hollow-sphere porous carbon derived from puffball spores for high performance supercapacitors. *Appl. Surf. Sci.* **2020**, *542*, 148697. [CrossRef]
211. Gao, X.; Li, X.; Kong, Z.; Xiao, G.; Zhu, Y. Bifunctional 3D n-doped porous carbon materials derived from paper towel for oxygen reduction reaction and supercapacitor. *Sci. Bull.* **2018**, *63*, 621–628. [CrossRef]
212. Ma, G.; Yang, Q.; Sun, K.; Peng, H.; Ran, F.; Zhao, X.; Lei, Z. Nitrogen-doped porous carbon derived from biomass waste for high-performance supercapacitor. *Bioresour. Technol.* **2015**, *197*, 137–142. [CrossRef]
213. Guan, L.; Pan, L.; Peng, T.; Gao, C.; Zhao, W.; Yang, Z.; Hu, H.; Wu, M. Synthesis of biomass-derived nitrogen-doped porous carbon nanosheests for high-performance supercapacitors. *ACS Sustain. Chem. Eng.* **2019**, *7*, 8405–8412. [CrossRef]
214. Chen, H.; Liu, D.; Shen, Z.; Bao, B.; Zhao, S.; Wu, L. Functional biomass carbons with hierarchical porous structure for supercapacitor electrode materials. *Electrochim. Acta* **2015**, *180*, 241–251. [CrossRef]
215. Zhao, G.; Li, Y.; Zhu, G.; Shi, J.; Lu, T.; Pan, L. Biomass-based N, P, and S self-doped porous carbon for high-performance supercapacitors. *ACS Sustain. Chem. Eng.* **2019**, *7*, 12052–12060. [CrossRef]
216. Loow, Y.-L.; Wu, T.Y.; Yang, G.H.; Jahim, J.M.; Teoh, W.H.; Mohammad, A.W. Role of energy irradiation in aiding pretreatment of lignocellulosic biomass for improving reducing sugar recovery. *Cellulose* **2016**, *23*, 2761–2789. [CrossRef]
217. Bai, P.; Wei, S.; Lou, X.; Xu, L. An ultrasound-assisted approach to bio-derived nanoporous carbons: Disclosing a linear relationship between effective micropores and capacitance. *RSC Adv.* **2019**, *9*, 31447–31459. [CrossRef] [PubMed]
218. Kokai, F.; Sorin, R.; Chigusa, H.; Hanai, K.; Koshio, A.; Ishihara, M.; Koga, Y.; Hasegawa, M.; Imanishi, N.; Takeda, Y. Ultrasonication fabrication of high quality multilayer graphene flakes and their characterization as anodes for lithium ion batteries. *Diam. Relat. Mater.* **2012**, *29*, 63–68. [CrossRef]
219. Zhou, G.; Yin, J.; Sun, Z.; Gao, X.; Zhu, F.; Zhao, P.; Li, R.; Xu, J. An ultrasonic-assisted synthesis of rice-straw-based porous carbon with high performance symmetric supercapacitors. *RSC Adv.* **2020**, *10*, 3246–3255. [CrossRef]
220. Thiemann, A.; Holsteyns, F.; Cairós, C.; Mettin, R. Sonoluminescence and dynamics of cavitation bubble populations in sulfuric acid. *Ultrason. Sonochem.* **2017**, *34*, 663–676. [CrossRef] [PubMed]
221. Gireesan, S.; Pandit, A.B. Modeling the effect of carbon-dioxide gas on cavitation. *Ultrason. Sonochem.* **2017**, *34*, 721–728. [CrossRef]
222. Merouani, S.; Hamdaoui, O.; Rezgui, Y.; Guemini, M. Theoretical estimation of the temperature and pressure within collapsing acoustical bubbles. *Ultrason. Sonochem.* **2014**, *21*, 53–59. [CrossRef]
223. Feng, L.; Cao, Y.; Xu, D.; Wang, S.; Zhang, J. Molecular weight distribution, rheological property and structural changes of sodium alginate induced by ultrasound. *Ultrason. Sonochem.* **2017**, *34*, 609–615. [CrossRef] [PubMed]
224. Leng, C.; Sun, K.; Li, J.; Jiang, J. The reconstruction of char surface by oxidized quantum-size carbon dots under the ultrasonic energy to prepare modified activated carbon materials as electrodes for supercapacitors. *J. Alloys Compd.* **2017**, *714*, 443–452. [CrossRef]
225. Chen, F.; Ji, Y.; Deng, Y.; Ren, F.; Tan, S.; Wang, Z. Ultrasonic-assisted fabrication of porous carbon materials derived from agricultural waste for solid-state supercapacitors. *J. Mater. Sci.* **2020**, *55*, 11512–11523. [CrossRef]
226. Wang, T.; Li, G.; Yang, K.; Zhang, X.; Wang, K.; Cai, J.; Zheng, J. Enhanced ammonium removal on biochar from a new forestry waste by ultrasonic activation: Characteristics, mechanisms and evaluation. *Sci. Total Environ.* **2021**, *778*, 146295. [CrossRef]
227. James, S.L.; Adams, C.J.; Bolm, C.; Braga, D.; Collier, P.; Friščić, T.; Grepioni, F.; Harris, K.D.M.; Hyett, G.; Jones, W.; et al. Mechanochemistry: Opportunities for new and cleaner synthesis. *Chem. Soc. Rev.* **2011**, *41*, 413–447. [CrossRef] [PubMed]
228. Panchal, M.; Raghavendra, G.; Ojha, S.; Omprakash, M.; Acharya, S.K. A single step process to synthesize ordered porous carbon from coconut shells-eggshells biowaste. *Mater. Res. Express* **2019**, *6*, 115613. [CrossRef]
229. Du, J.; Zhang, Y.; Lv, H.; Chen, A. N/B-co-doped ordered mesoporous carbon spheres by ionothermal strategy for enhancing supercapacitor performance. *J. Colloid Interface Sci.* **2021**, *587*, 780–788. [CrossRef]
230. Mehdi, R.; Raza, N.; Naqvi, S.R.; Khoja, A.H.; Mehran, M.T.; Farooq, M.; Tran, K.-Q. A comparative assessment of solid fuel pellets production from torrefied agro-residues and their blends. *J. Anal. Appl. Pyrolysis* **2021**, *156*, 105125. [CrossRef]
231. Zhang, W.; Liang, M.; Lu, C. Morphological and structural development of hardwood cellulose during mechanochemical pretreatment in solid state through pan-milling. *Cellulose* **2007**, *14*, 447–456. [CrossRef]

232. Liu, H.; Zhang, Y.; Hou, T.; Chen, X.; Gao, C.; Han, L.; Xiao, W. Mechanical deconstruction of corn stover as an entry process to facilitate the microwave-assisted production of ethyl levulinate. *Fuel Process. Technol.* **2018**, *174*, 53–60. [CrossRef]
233. Zakaria, M.R.; Fujimoto, S.; Hirata, S.; Hassan, M.A. Ball milling pretreatment of oil palm biomass for enhancing enzymatic hydrolysis. *Appl. Biochem. Biotechnol.* **2014**, *173*, 1778–1789. [CrossRef]
234. Mattonai, M.; Pawcenis, D.; del Seppia, S.; Łojewska, J.; Ribechini, E. Effect of ball-milling on crystallinity index, degree of polymerization and thermal stability of cellulose. *Bioresour. Technol.* **2018**, *270*, 270–277. [CrossRef]
235. Shen, F.; Sun, S.; Yang, J.; Qiu, M.; Qi, X. Coupled pretreatment with liquid nitrogen and ball milling for enhanced cellulose hydrolysis in water. *ACS Omega* **2019**, *4*, 11756–11759. [CrossRef]
236. Khan, A.S.; Man, Z.; Bustam, M.A.; Kait, C.F.; Khan, M.I.; Muhammad, N.; Nasrullah, A.; Ullah, Z.; Ahmad, P. Impact of ball-milling pretreatment on pyrolysis behavior and kinetics of crystalline cellulose. *Waste Biomass Valorization* **2015**, *7*, 571–581. [CrossRef]
237. Lin, X.; Liang, Y.; Lu, Z.; Lou, H.; Zhang, X.; Liu, S.; Zheng, B.; Liu, R.; Fu, R.; Wu, D. Mechanochemistry: A green, activation-free and top-down strategy to high-surface-area carbon materials. *ACS Sustain. Chem. Eng.* **2017**, *5*, 8535–8540. [CrossRef]
238. Shen, F.; Qiu, M.; Hua, Y.; Qi, X. Dual-Functional Templated Methodology for the Synthesis of Hierarchical Porous Carbon for Supercapacitor. *ChemistrySelect* **2018**, *3*, 586–591. [CrossRef]
239. Bahuguna, A.; Kumar, A.; Krishnan, V. carbon-support-based heterogeneous nanocatalysts: Synthesis and applications in organic reactions. *Asian J. Org. Chem.* **2019**, *8*, 1263–1305. [CrossRef]
240. Shan, D.; Deng, S.; Zhao, T.; Wang, B.; Wang, Y.; Huang, J.; Yu, G.; Winglee, J.; Wiesner, M.R. Preparation of ultrafine magnetic biochar and activated carbon for pharmaceutical adsorption and subsequent degradation by ball milling. *J. Hazard. Mater.* **2015**, *305*, 156–163. [CrossRef] [PubMed]
241. Filiciotto, L.; Balu, A.M.; Romero, A.A.; Rodríguez-Castellón, E.; van der Waal, J.C.; Luque, R. Benign-by-design preparation of humin-based iron oxide catalytic nanocomposites. *Green Chem.* **2017**, *19*, 4423–4434. [CrossRef]
242. Shi, Y.; Liu, X.; Wang, M.; Huang, J.; Jiang, X.; Pang, J.; Xu, F.; Zhang, X. Synthesis of N-doped carbon quantum dots from bio-waste lignin for selective irons detection and cellular imaging. *Int. J. Biol. Macromol.* **2019**, *128*, 537–545. [CrossRef]
243. Tran, T.H.; Nguyen, H.-L.; Hao, L.T.; Kong, H.; Park, J.M.; Jung, S.-H.; Gil Cha, H.; Lee, J.Y.; Kim, H.; Hwang, S.Y.; et al. A ball milling-based one-step transformation of chitin biomass to organo-dispersible strong nanofibers passing highly time and energy consuming processes. *Int. J. Biol. Macromol.* **2018**, *125*, 660–667. [CrossRef]
244. Peterson, S.C.; Jackson, M.A.; Kim, S.; Palmquist, D.E. Increasing biochar surface area: Optimization of ball milling parameters. *Powder Technol.* **2012**, *228*, 115–120. [CrossRef]
245. Lyu, H.; Gao, B.; He, F.; Zimmerman, A.R.; Ding, C.; Huang, H.; Tang, J. Effects of ball milling on the physicochemical and sorptive properties of biochar: Experimental observations and governing mechanisms. *Environ. Pollut.* **2018**, *233*, 54–63. [CrossRef]
246. Rajendiran, R.; Nallal, M.; Park, K.H.; Li, O.L.; Kim, H.-J.; Prabakar, K. Mechanochemical assisted synthesis of heteroatoms inherited highly porous carbon from biomass for electrochemical capacitor and oxygen reduction reaction electrocatalysis. *Electrochim. Acta* **2019**, *317*, 1–9. [CrossRef]
247. Huang, L.; Wu, Q.; Liu, S.; Yu, S.; Ragauskas, A.J. Solvent-free production of carbon materials with developed pore structure from biomass for high-performance supercapacitors. *Ind. Crop. Prod.* **2020**, *150*, 112384. [CrossRef]
248. Teng, Z.; Han, K.; Li, J.; Gao, Y.; Li, M.; Ji, T. Ultrasonic-assisted preparation and characterization of hierarchical porous carbon derived from garlic peel for high-performance supercapacitors. *Ultrason. Sonochem.* **2020**, *60*, 104756. [CrossRef] [PubMed]